

Influence of non-local diffusion in avascular tumour growth

Original

Influence of non-local diffusion in avascular tumour growth / Ramírez-Torres, Ariel; Di Stefano, Salvatore; Grillo, Alfio. - In: MATHEMATICS AND MECHANICS OF SOLIDS. - ISSN 1081-2865. - STAMPA. - 26:9(2021), pp. 1264-1293. [10.1177/1081286520975086]

Availability:

This version is available at: 11583/2863595 since: 2022-01-18T12:15:26Z

Publisher:

Sage

Published

DOI:10.1177/1081286520975086

Terms of use:

This article is made available under terms and conditions as specified in the corresponding bibliographic description in the repository

Publisher copyright

Sage postprint/Author's Accepted Manuscript

Ramírez-Torres, Ariel; Di Stefano, Salvatore; Grillo, Alfio, Influence of non-local diffusion in avascular tumour growth, accepted for publication in MATHEMATICS AND MECHANICS OF SOLIDS (26 9) pp. 1264-1293. © 2021 (Copyright Holder). DOI:10.1177/1081286520975086

(Article begins on next page)

Influence of non-local diffusion in avascular tumour growth*

Ariel Ramírez-Torres^{1,2}, Salvatore Di Stefano¹, and Alfio Grillo¹

¹Dipartimento di Scienze Matematiche “G. L. Lagrange” Politecnico di
Torino, 10129. Torino, Italia

²School of Mathematics and Statistics, Mathematics and Statistics
Building, University of Glasgow, University Place, Glasgow G128QQ, UK

Abstract

The availability and evolution of chemical agents play an important role in the growth of a tumour and, therefore, the mathematical description of their consumption is of special interest. Usually, Fick’s law of diffusion is adopted for describing the local character of the evolution of chemicals. However, in a highly complex, heterogeneous medium, as is a tumour, the progression of chemical species could be influenced by non-local interactions. In this respect, our goal is to investigate the influence of such type of diffusion on the growth of a tumour in avascular stage. For our purposes, we consider a diffusion equation for the evolution of the chemical agents that accounts for the existence of non-local interactions in a non-Fickian manner, and that involves notions of Fractional Calculus. In particular, the introduction of derivatives or integrals of fractional type of order $\alpha \in \mathbb{R}$ has proven to be an effective mathematical tool in the description of various non-local phenomena. To achieve our goals, we adopt part of the modelling assumptions outlined in previous works of the authors, in which the growth of a tumour is described in terms of mass transfer among the tumour’s constituents and structural changes that occur in the tumour itself in response to growth. The latter ones are characterised by means of the Bilby–Kröner–Lee decomposition of the deformation gradient tensor. We perform numerical simulations, whose results indicate the relevance of embracing a fractional framework in modelling tumour growth. Specifically, the real parameter α “dominates” the way in which the tumour grows, since it permits to model a variety of growth patterns ranging from the standard growth to no growth at all.

Keywords Tumour growth, non-Fickian diffusion, non-local interactions, inelastic distortions

*The final version of this article has been accepted for publication by Sage Journals, it is available online at “<https://journals.sagepub.com/doi/10.1177/1081286520975086>” and should be cited as: “Ramírez-Torres A, Di Stefano S, Grillo A. Influence of non-local diffusion in avascular tumour growth. *Mathematics and Mechanics of Solids*. January 2021. doi:10.1177/1081286520975086”

1 Introduction

For several years now, the scientific literature has experienced an important increase in the mathematical modelling of tumour growth (see e.g. [20, 14, 8, 64, 100, 78, 7, 107, 66, 97, 65] and the references therein). However, there is still the necessity for understanding the connections among the different processes of chemical, biological and/or mechanical nature that take place at different time and length scales and influence the evolution of a tumour.

From the mechanical perspective, the growth of a tumour is closely related to the appearance of transformations of its internal structure that arise in response to mass changes, which may be driven by its chemo-mechanical environment and coexist with the “*visible*” deformation of the tumour itself [39, 32, 95]. An important feature of this phenomenology is that the structural transformations are often accompanied by the production of residual stresses [98, 72, 52, 28, 101]. In this respect, we mention the series of experiments conducted by Stylianopoulos et al. [110] on tumour spheroids, which indicate the existence of an incompatible, stress-free state for such systems and, thus, suggest to interpret growth in terms of inelastic distortions in addition to mere changes of shape. This conclusion permits to invoke the Bilby–Kröner–Lee (BKL) multiplicative decomposition of the deformation gradient tensor [85, 52, 102]. As long as volumetric growth is concerned and, as in the case of the present work, no other types of structural transformations are accounted for, the BKL decomposition reduces to decomposing the deformation gradient tensor into two contributions. One is related to the changes of the tissue’s internal structure due to the gain or loss of mass, and the other one to distortions of purely elastic nature (note that, here and in the sequel, we shall use the terms “tumour” and “tissue” interchangeably). We refer to the works [102, 52, 94, 27, 101, 56], and to the references therein, for a more complete discussion on the BKL multiplicative decomposition.

It is worth noting that, although the inelastic distortions accompanying growth play an important role on its evolution [61, 6, 4, 51, 80], which may also be partially self-driven [41, 101], it is clear that the growth of a tumour is strongly conditioned by the presence of chemical agents of various nature, such as nutrients. Therefore, in order to elaborate a model of tumour growth, it is crucial to be able to model the evolution of chemical substances. Fick’s law of diffusion is largely adopted for this purpose, even though it has often turned out to be inconsistent with the results of some observed transport processes [48, 21, 31], which are thus referred to as *non-Fickean*. In fact, non-Fickean diffusion processes have been recognised in several biological tissues, including cells [48, 31], neuromuscular junctions [74] and brain tissue [21], among others. In particular, the experiments conducted by Danyuo et al. [34] suggest that cancer drug release kinetics in breast cancer is non-Fickean.

A common characteristic of the occurrence of non-Fickean patterns, as suggested in several works [73, 84, 48, 67, 45], is the multi-scale and heterogeneous nature of the environment in which diffusion takes place. Specifically, Lacks [74] shows that geometric factors, such as tortuosity, could cause the diffusion processes occurring in a neuromuscular junction to be non-Fickean. Within this view, in the case of a tumour, although to our knowledge there is no experimental evidence that correlates non-Fickean diffusion with its internal structure, its microvascular network is known to have a strong influence on transport phenomena. In fact, this issue has been discussed in several papers, like e.g. [69, 90] and references therein.

In general, non-Fickean behaviours can be gathered in two categories:

- (i) non-locality in time, which associates the mass flux of a given chemical agent with the

68 concentration gradient of that agent through an integro-differential relationship, such as, for
69 example, those involving fractional time derivatives or fractional time integrals [9];

- 70 (ii) non-locality in space, which means that the mass flux vector of a species *cannot* be expressed
71 as a point-wise linear function of the concentration gradient, as Fick’s law would prescribe.

72 In this work, we focus on the second type of non-locality, and we are interested in quantifying
73 the spatial influence of the mass flux at a given point on “distant” points of a body. However, it
74 is important to recall that non-locality is a broad notion [43, 47], which covers a wide spectrum
75 of phenomena, from transport processes [44] to plasticity [2, 57] or visco-elasticity [10, 37], and
76 depends on the intrinsic structure of the system to which it is referred and/or on its response to
77 long-range stimuli. Moreover, non-locality can be introduced in different ways, e.g., by having
78 recourse to higher-order gradient theories, as is the case for plasticity [2, 57, 109], or by assigning
79 constitutive laws that feature integro-differential operators [71, 43]. In particular, the employment
80 of integrals and derivatives of fractional order [92, 9, 12] has demonstrated to be an effective method
81 in the description of various non-local phenomena [11, 18, 22], including non-Fickian diffusion
82 [26, 82, 35, 86]. As pointed out in [35], the introduction of Fractional Calculus allows for the
83 description of non-Fickian transport processes in a natural way, because of their close connection
84 with the concept of anomalous diffusion [84].

85 Before going further, we notice that in the literature there exist other non-Fickian diffusion
86 laws that, however, do not rely on the assumption of non-local effects. In particular, the Maxwell-
87 Stefan model [70], which generalises Fick’s diffusion by the consideration of “*thermodynamic non-*
88 *idealities*”¹ and “*influence of external force fields*”, has been postulated in the study of porous
89 media and tumour growth [68].

90 1.1 Aim and novelties of our work

91 In the present work, on the basis of the indications given above, our aim is to highlight and
92 study the influence of the non-local character of diffusion processes that could be acting in an
93 avascular tumour. To accomplish this task, we propose a potentially new constitutive relationship
94 of fractional type for the mass flux vector. Consequently, we refer only to fractional operators in
95 space, so that the model is non-local in space but local in time. In our formulation, the mass flux
96 vector of the chemical species, evaluated at a given spatial point, is put in relation, through an
97 integral operator, to the concentration gradient of that species, evaluated at all other points of
98 the region of space occupied by the tumour. This leads to a generalisation of Fick’s law that can
99 be related to Fractional Calculus in a straightforward manner. In particular, this connection will
100 become evident in the specification of the mass flux vector for the study of a benchmark problem
101 (see Section “Definition of the non-locality function”).

102 For our purposes, we adopt part of the modelling assumptions outlined in [80, 101, 56, 91].
103 Specifically, we study the tumour as a mixture comprising a fluid phase and a solid phase, and we
104 identify its growth with the gain or loss of mass of the solid phase at the expenses or advantage of

¹According to [115], the thermodynamic non-idealities are related to a phenomenon that pertains to a thermodynamic system, like, for instance, a gas, and that occurs through the “*storage of potential energy*” among the molecules of the system itself as a result of the interactions among such molecules. The main consequence of the non-idealities is that the concentrations of the molecules turn out to be different from those expected in the absence of the energy storage among them.

105 the fluid one. In particular, the model we employ predicts the gain of mass for a sufficiently high
106 concentration of chemical agents (in fact, nutrients) and the loss of mass when the concentration
107 of these falls below a certain threshold [81, 80]. Moreover, in the case of mass uptake of the solid
108 phase, the model accounts for mechanotransduction [81, 80, 50, 56], thereby allowing a modulation
109 of growth by means of stress [81, 80], whereas both for positive and for negative growth, the onset of
110 structural transformations and their related inelastic distortions are considered. In the remainder
111 of this work, we address only the most pertinent considerations and equations, while we refer the
112 Reader to [80, 101, 91] for further details.

113 Before going further, we find it convenient to highlight the main novelties of our work, which
114 can be summarised as follows:

- 115 1. *Impact of non-local diffusion on tumour growth.* With respect to [80, 101, 56, 91], we study the
116 diffusion of the chemical agents in a growing tumour by hypothesising a non-local constitutive
117 law for the diffusive mass flux vector. This is done with the purpose of weighing how and to
118 which extent the deviation of non-local diffusion from the Fickian one impacts on the main
119 descriptors of the tumour's evolution.
- 120 2. *Evolving non-locality driven by the tumour's dynamics.* The model that we are proposing
121 requires to solve a type of non-locality that changes with the dynamics of the tumour through
122 its motion *and* growth. To the best of our knowledge, this is a generalisation of a setting
123 adopted in several papers (see e.g. [35, 63, 105, 75]), where the non-locality is accounted for
124 in advection-diffusion equations without considering the deformation or structural change of
125 the media in which such equations are defined.
- 126 3. *Non-locality and non-linearity.* The core of our work is the equation governing the evolution
127 of chemical agents. This is given by an advection-diffusion-reaction equation featuring a
128 fractional diffusive mass flux vector and a non-linear reaction term. We solve this equation
129 *together* with all the other balance laws, expressed by non-linear partial differential equations,
130 that model the tumour and its growth. Therefore, we solve a system of equations in which
131 non-linearity combines with non-locality. To us, this is a novelty because, to the best of our
132 knowledge, papers on Fractional Calculus usually solve one equation in conjunction with a
133 fractional constitutive law. Furthermore, the nature of the problem we are tackling makes it
134 impossible to have recourse to solution techniques based on Fourier and Laplace transforms,
135 which are standard for problems of Fractional Calculus that are linear and/or formulated in
136 unbounded domains. In our case, however, this assumption would be physically unrealistic
137 and we have, thus, to turn to numerical techniques, such as Finite Element (FE) methods.

138 We point out that the study of fractional diffusion in bounded domains is delicate because
139 of the complexity of the numerics involving operators of fractional type. Nevertheless, in the
140 literature there exist some works dealing with fractional diffusion equations on bounded domains.
141 The majority of these works employ finite-difference Grünwald-Letnikov discretisation schemes
142 (see e.g. [88, 76, 36, 83]), and there also exist studies in which FE methods have been used for
143 solving equations of fractional type [99, 63, 49, 44]. However, to the best of our knowledge, there
144 is still a lack of studies addressing in detail the numerical issues arising in the context of fractional
145 differential equations within a non-linear mechanical framework.

146 We also mention that, in this work, we suggest a possible way of formulating non-local diffusion
147 on manifolds by adapting the definition of convolution on manifolds given in [106]. Originally, we

148 encountered the necessity of expressing convolution in the non-Euclidean context because we aimed
 149 at writing our model in fully covariant formalism as a first step towards non-Euclidean settings.
 150 However, we faced some technical difficulties, which made us opt, for the time being, to give just a
 151 sketch of the generalisation of non-local diffusion on manifolds. For this reason, we summarised the
 152 main steps of our generalisation in Appendix A1. Note that Meerschaert et al. [82] did consider
 153 diffusion-like problems on manifolds but within a different framework.

154 Finally, we would like to point out that, throughout this work, the terminologies “mass fraction”
 155 and “concentration” will be often used interchangeably, and the spatial and temporal dependence
 156 of the variables are dropped out, unless there is a necessity to account for the non-local character
 157 of the problem, where this dependence is explicitly specified.

158 2 Kinematics

159 Let \mathcal{S} be the three-dimensional Euclidean space, \mathcal{T} an interval of time, and $\mathcal{B} \subset \mathcal{S}$ the reference
 160 placement of the mechanical system representing an avascular tumour, in which the tumour may,
 161 or may not, be free of stress. In particular, we consider that the tumour is a saturated mixture
 162 comprising a solid and a fluid phase. Moreover, the region of \mathcal{S} occupied by the system at time
 163 $t \in \mathcal{T}$ is referred to as current configuration and is denoted by $\mathcal{B}_t \equiv \chi(\mathcal{B}, t)$, where $\chi(\cdot, t) : \mathcal{B} \rightarrow \mathcal{S}$
 164 describes the motion of the solid phase (for the mixture kinematics, we follow here the same
 165 approach as the one adopted in [33]). Then, a point $x \in \mathcal{B}_t$ is given by $x = \chi(X, t)$, with
 166 $X \in \mathcal{B}$ and $t \in \mathcal{T}$. By differentiating the motion χ with respect to X , we obtain the deformation
 167 gradient tensor, \mathbf{F} , defined as the tangent map of χ , i.e., $\mathbf{F}(\cdot, t) \equiv T\chi(\cdot, t) : T\mathcal{B} \rightarrow T\mathcal{S}$,
 168 with $T\mathcal{B} = \sqcup_{X \in \mathcal{B}} T_X \mathcal{B}$ and $T\mathcal{S} = \sqcup_{x \in \mathcal{S}} T_x \mathcal{S}$. Thus, tensor $\mathbf{F}(X, t)$ characterises the visible
 169 deformations of the system by mapping vectors of the tangent space $T_X \mathcal{B}$ into the tangent space
 170 $T_x \mathcal{S}$.

171 We also introduce the spatial volumetric fractions of the solid and the fluid phases, given by
 172 $\varphi_s(x, t)$ and $\varphi_f(x, t)$, respectively. Then, we define the *apparent* mass densities, $\varphi_s(x, t)\varrho_s(x, t)$ and
 173 $\varphi_f(x, t)\varrho_f(x, t)$, of the solid and of the fluid, where $\varrho_s(x, t)$ and $\varrho_f(x, t)$ represent the *true* mass
 174 densities of the solid and the fluid phase, respectively. We notice that the apparent mass densities
 175 express, in each case, the phase mass per unit volume of the mixture as a whole, whereas each true
 176 mass density is the inherent density of the corresponding phase. Furthermore, the saturation of
 177 the mixture implies that $\varphi_s(x, t) + \varphi_f(x, t) = 1$, for all $x \in \mathcal{B}_t$ and $t \in \mathcal{T}$.

178 The velocity of the mixture is $\mathbf{v}(x, t) := \sum_{k \in \{s, f\}} \varphi_k(x, t)\varrho_k(x, t)\mathbf{v}_k(x, t)/\varrho(x, t)$, where $\mathbf{v}_s(x, t)$
 179 and $\mathbf{v}_f(x, t)$ denote the velocities of the solid and the fluid phases, respectively, and $\varrho(x, t) :=$
 180 $\sum_{k \in \{s, f\}} \varphi_k(x, t)\varrho_k(x, t)$ is the mass density of the mixture as a whole. We notice that, by intro-
 181 ducing the solid phase velocity $\mathbf{V}_s(X, t) := \dot{\chi}(X, t)$, where the “dot” symbol denotes differentiation
 182 with respect to time, the relationship $\mathbf{v}_s(x, t) = \mathbf{v}_s(\chi(X, t), t) = \mathbf{V}_s(X, t)$ holds true for all $X \in \mathcal{B}$
 183 and $t \in \mathcal{T}$. Furthermore, since the tumour under study is assumed to be a mixture also in \mathcal{B} ,
 184 the solid and the fluid coexist at every point $X \in \mathcal{B}$. This situation implies that any point x in
 185 the fluid phase can be also viewed as the image of X through the motion χ and, consequently,
 186 $\mathbf{v}_f(x, t) = \mathbf{v}_f(\chi(X, t), t) = \mathbf{V}_f(X, t)$.

187 2.1 Kinematics of growth

188 As suggested in several works, see e.g. [46, 110] and references therein, a relevant feature in the
 189 growth of a tumour is the manifestation of irreversible changes of its internal structure. To take
 190 this aspect into account, we employ some concepts taken from the theory of inelastic processes.
 191 Specifically, for characterising the growth of the tissue under study, we invoke the Bilby-Kröner-Lee
 192 (BKL) decomposition of the deformation gradient tensor [85, 27, 102, 98, 52], i.e.,

$$\mathbf{F} = \mathbf{F}_e \mathbf{F}_\gamma, \quad (1)$$

193 where the generally non-integrable tensor fields \mathbf{F}_e and \mathbf{F}_γ describe the elastic accommodation of
 194 the tumour and the inelastic distortions induced by growth, respectively. We denote by $\mathcal{N}_t(X)$
 195 the *natural state* of the body element of the tumour's solid phase associated with X , and we let
 196 it represent a stress-free state. We refer to the tensor $\mathbf{F}_\gamma(X, t): T_X \mathcal{B} \rightarrow \mathcal{N}_t(X)$ as *growth tensor*
 197 and we assume that it comprehends the structural transformations undergone by the tumour in the
 198 course of its evolution. Then, the accommodating elastic tensor $\mathbf{F}_e(X, t)$ maps vectors of $\mathcal{N}_t(X)$
 199 into vectors of $T_x \mathcal{S}$. We refer to the works [102, 52, 94, 27, 101, 56], and references therein, for a
 200 more complete discussion on the nature and generalisation of the multiplicative decomposition in
 201 Equation (1).

202 In particular, following [80, 101, 56], in the present work we contemplate the case in which the
 203 growth tensor is a pure dilatation, that is, we impose $\mathbf{F}_\gamma = \gamma \mathbf{I}$, where $\gamma > 0$ is referred to as *growth*
 204 *parameter* and \mathbf{I} is the second-order identity tensor.

205 3 Balance laws

206 By adopting the modelling assumptions made in [80, 101, 56], we consider that the fluid phase is
 207 constituted by chemical agents and “water”, with mass fractions c_a and c_w , respectively, and such
 208 that $c_a + c_w = 1$. Furthermore, we hypothesise the solid phase to consist of two type of cells, i.e.,
 209 the proliferating cells, with mass fraction c_p , and the necrotic cells, with mass fraction c_n , where
 210 $c_p + c_n = 1$.

211 3.1 Mass balance laws

212 The mass balance laws for the gain and loss of mass of the proliferating and the necrotic cells, and
 213 for the mass fraction of the chemical species and the fluid phase as a whole are

$$\partial_t(\varphi_s \varrho_s c_p) + \operatorname{div}(\varphi_s \varrho_s c_p \mathbf{v}_s) = r_{\text{pn}} + r_{\text{fp}}, \quad (2a)$$

$$\partial_t(\varphi_s \varrho_s c_n) + \operatorname{div}(\varphi_s \varrho_s c_n \mathbf{v}_s) = r_{\text{nf}} - r_{\text{pn}}, \quad (2b)$$

$$\partial_t(\varphi_f \varrho_f c_a) + \operatorname{div}(\varphi_f \varrho_f c_a \mathbf{v}_f + \mathbf{y}_\alpha) = r_{\text{ap}}, \quad (2c)$$

$$\partial_t(\varphi_f \varrho_f) + \operatorname{div}(\varphi_f \varrho_f \mathbf{v}_f) = -r_s, \quad (2d)$$

214 where r_{pn} , r_{fp} , r_{nf} and r_{ap} denote rates of mass intake and/or reduction [80, 101, 56]. Specifically,
 215 they represent the rate at which the proliferating cells turn into necrotic (r_{pn}), the mass from the
 216 fluid phase that promotes the proliferation of cells (r_{fp}), the necrotic cells that dissolve into the
 217 fluid (r_{nf}), and the chemical agents that are depleted by the proliferating cells (r_{ap}). Moreover,

218 $r_s := r_{\text{fp}} + r_{\text{nf}}$ is the global source/sink of mass of the solid phase as a whole. Particularly, in
 219 writing Equations (2a) and (2b), we have enforced the consideration that the two cell populations
 220 move at the same velocity \mathbf{v}_s . In Equation (2c), the term \mathbf{y}_α corresponds to the mass flux vector
 221 of the chemical agents, and since the focus of this work is subordinate to its definition, we prefer
 222 to make a deeper analysis of its characterisation and physical meaning in a separate section.

223 By enforcing that the tissue's cells are mainly composed by water [19, 80, 51], the true mass
 224 density of the solid phase, ϱ_s , can be regarded as constant and equal to the true mass density of the
 225 fluid phase, ϱ_f , which is set to be equal to the density of water. Thus, by taking into account the
 226 saturation constraint and the BKL decomposition in Equation (1), Equations (2a)–(2d), written
 227 with respect to the reference configuration, become

$$\dot{\mathbf{c}}_p = [R_{\text{pn}} + R_{\text{fp}} - R_s \mathbf{c}_p][J_\gamma \Phi_{s\nu} \varrho_s]^{-1}, \quad (3a)$$

$$\frac{\dot{\gamma}}{\gamma} = [R_{\text{fp}} + R_{\text{nf}}][3\varrho_s \Phi_{s\nu} J_\gamma]^{-1}, \quad (3b)$$

$$\varrho_f [J - J_\gamma \Phi_{s\nu}] \dot{\mathbf{c}}_a + \varrho_f \mathbf{Q} \text{Grad} \mathbf{c}_a + \text{Div} \mathbf{Y}_\alpha = \mathbf{c}_a R_s + R_{\text{ap}}, \quad (3c)$$

$$\text{Div} \mathbf{Q} + \dot{J} = 0, \quad (3d)$$

228 where the material filtration velocity \mathbf{Q} , the material mass flux vector of the chemical agents \mathbf{Y}_α , the
 229 mass fractions \mathbf{c}_a and \mathbf{c}_p , and the material sources/sinks of mass featuring in Equations (3a)–(3d)
 230 are given by

$$\mathbf{Q}(X, t) := J(X, t) \mathbf{q}(\chi(X, t), t) \mathbf{F}^{-\text{T}}(X, t), \quad (4a)$$

$$\mathbf{Y}_\alpha(X, t) := J(X, t) \mathbf{y}_\alpha(\chi(X, t), t) \mathbf{F}^{-\text{T}}(X, t), \quad (4b)$$

$$\mathbf{c}_k(X, t) := c_k(\chi(X, t), t), \quad k \in \{a, p\} \quad (4c)$$

$$R_\beta(X, t) := J(X, t) r_\beta(\chi(X, t), t), \quad \beta \in \{\text{pn}, \text{fp}, \text{nf}, \text{ap}, \text{s}\}, \quad (4d)$$

231 with $\mathbf{q} = \varphi_f [\mathbf{v}_f - \mathbf{v}_s]$. We note that, in writing Equations (3a)–(3d), the material volumetric
 232 fractions $\Phi_s(X, t) := J(X, t) \varphi_s(\chi(X, t), t)$ and $\Phi_f(X, t) := J(X, t) \varphi_f(\chi(X, t), t)$ have been written
 233 as $\Phi_s = J_\gamma \Phi_{s\nu}$ and $\Phi_f = J - J_\gamma \Phi_{s\nu}$, where $\Phi_{s\nu}(X, t) := J_e(X, t) \varphi_s(\chi(X, t), t)$ is the “pull-back” of
 234 the solid phase volumetric fraction, φ_s , to the natural state [101, 56]. In particular, by imposing
 235 that the temporal derivative of J_γ compensates for the mass source r_s [42, 5], it can be deduced
 236 that the volumetric fraction $\Phi_{s\nu}$ is independent of time. However, $\Phi_{s\nu}$ may depend on material
 237 points [56]. Furthermore, since it holds true that $J_e = J/J_\gamma$, the volumetric fractions of the solid
 238 and the fluid phase can be expressed entirely in terms of the volume ratios J and J_γ , i.e.,

$$\varphi_s(x, t) = \varphi_s(\chi(X, t), t) = \frac{J_\gamma(X, t) \Phi_{s\nu}(X)}{J(X, t)}, \quad (5a)$$

$$\varphi_f(x, t) = 1 - \varphi_s(x, t) = \frac{J(X, t) - J_\gamma(X, t) \Phi_{s\nu}(X)}{J(X, t)}. \quad (5b)$$

239 3.2 Momentum balance laws

240 In this work, we neglect inertial and body forces, so that the momentum balance laws for the
 241 biphasic medium as a whole and for the fluid phase write [60, 54, 91]

$$\text{div}(\boldsymbol{\sigma}_s + \boldsymbol{\sigma}_f) = \mathbf{0}, \quad (6a)$$

$$\mathbf{q} = -\mathbf{k} \operatorname{grad} p, \quad (6b)$$

where $\boldsymbol{\sigma}_s$ and $\boldsymbol{\sigma}_f$ are the Cauchy stress tensors of the solid and the fluid phase, p is the hydrostatic pressure, Equation (6b) expresses Darcy's law [60], and \mathbf{k} denotes the *permeability tensor*, which is here taken to be symmetric and positive definite.

Following [60, 15, 53, 101], we assume the fluid phase to be macroscopically inviscid, so that $\boldsymbol{\sigma}_f$ is purely hydrostatic, and we write

$$\boldsymbol{\sigma}_f = -\varphi_f p \mathbf{g}^{-1}, \quad (7a)$$

$$\boldsymbol{\sigma}_s = -\varphi_s p \mathbf{g}^{-1} + \boldsymbol{\sigma}_{sc}, \quad (7b)$$

where $\boldsymbol{\sigma}_{sc}$ is said to be the constitutive part of $\boldsymbol{\sigma}_s$ and \mathbf{g}^{-1} is the inverse of the metric tensor, \mathbf{g} , associated with \mathcal{S} . Then, by substituting Equations (7a) and (7b) into Equation (6a), and performing the backward Piola transformation of Equations (6a) and (6b), we obtain

$$\operatorname{Div}(-J \mathbf{p} \mathbf{g}^{-1} \mathbf{F}^{-T} + \mathbf{P}_{sc}) = \mathbf{0}, \quad (8a)$$

$$\mathbf{Q} = -\mathbf{K} \operatorname{Grad} \mathbf{p}, \quad (8b)$$

where we have introduced the notation

$$\mathbf{p}(X, t) := p(\chi(X, t), t), \quad (9a)$$

$$\mathbf{K}(X, t) := J(X, t) \mathbf{F}^{-1}(\chi(X, t), t) \mathbf{k}(\chi(X, t), t) \mathbf{F}^{-T}(X, t), \quad (9b)$$

$$\mathbf{P}_{sc}(X, t) := J(X, t) \boldsymbol{\sigma}_{sc}(\chi(X, t), t) \mathbf{F}^{-T}(X, t), \quad (9c)$$

$$\mathbf{g}(X, t) := \mathbf{g}(\chi(X, t)), \quad (9d)$$

to denote, respectively, the pressure expressed as a function of time and of the points of \mathcal{B} , the material permeability tensor, the constitutive part of the overall first Piola-Kirchhoff stress tensor, and the metric tensor expressed as a function of time and of the points of \mathcal{B} . Moreover, Equation (8b) represents Darcy's law of filtration, pulled-back to the reference configuration.

4 Constitutive laws I: Strain energy density and permeability

Following [80, 101, 56], we hypothesise that the solid phase of the tumour is isotropic and hyperelastic, and introduce the strain energy densities \mathcal{W} and \mathcal{W}_ν , which are written per unit volume of the reference configuration and of the natural state, respectively. To account for the structural changes induced by growth, the strain energy density \mathcal{W} is expressed as a constitutive function, namely $\check{\mathcal{W}}$, depending on \mathbf{F} , \mathbf{F}_γ and on material points. Furthermore, we denote by $\check{\mathcal{W}}_\nu$ the constitutive representation of \mathcal{W}_ν , which is supposed here to depend solely on the tensor \mathbf{F}_e . Therefore, the following relationship holds [42, 30, 101]

$$\check{\mathcal{W}}(\mathbf{F}(X, t), \mathbf{F}_\gamma(X, t), X) = J_\gamma(X, t) \check{\mathcal{W}}_\nu(\mathbf{F}_e(X, t)). \quad (10)$$

Within a more general framework, the strain energy density $\check{\mathcal{W}}_\nu$ maintains the explicit dependence on X , and Equation (10) does not hold in its present form. This becomes evident when $\check{\mathcal{W}}_\nu$ is

parameterised by point-dependent material coefficients or, by expressing $\check{\mathcal{W}}_\nu$ as $\check{\mathcal{W}}_\nu = \Phi_{s\nu} \varrho_s \check{\Psi}_s$, where $\check{\Psi}_s$ is the solid phase strain energy density per unit mass, when $\Phi_{s\nu}$ depends on X . However, these circumstances are excluded from the setting of this work, as can be deduced by looking at Table 1, in which all the material parameters and $\Phi_{s\nu}$ are taken as constants.

Hereafter, we adopt a constitutive law of the type proposed in [62] for $\check{\mathcal{W}}_\nu$, i.e.,

$$\check{\mathcal{W}}_\nu(\mathbf{F}_e) = \hat{\mathcal{W}}_\nu(\mathbf{C}_e) = a_0 \{ \exp(\hat{\Psi}(\mathbf{C}_e)) - 1 \}, \quad (11a)$$

$$\hat{\Psi}(\mathbf{C}_e) = a_1 [\hat{I}_1(\mathbf{C}_e) - 3] + a_2 [\hat{I}_2(\mathbf{C}_e) - 3] - a_3 \log(\hat{I}_3(\mathbf{C}_e)), \quad (11b)$$

where $\hat{\mathcal{W}}_\nu$ is the constitutive representation of \mathcal{W} expressed as a function of the elastic, right Cauchy-Green deformation tensor $\mathbf{C}_e = \mathbf{F}_e^T \cdot \mathbf{F}_e = \mathbf{F}_\gamma^{-T} \mathbf{C} \mathbf{F}_\gamma^{-1}$, $\mathbf{C} = \mathbf{F}^T \cdot \mathbf{F}$ is the “classical”, right Cauchy-Green deformation tensor, $\hat{I}_1(\mathbf{C}_e) = \text{tr}(\mathbf{C}_e)$, $\hat{I}_2(\mathbf{C}_e) = \frac{1}{2} \{ [\hat{I}_1(\mathbf{C}_e)]^2 - \text{tr}[(\mathbf{C}_e)^2] \}$, and $\hat{I}_3(\mathbf{C}_e) = \det(\mathbf{C}_e)$ are the principal invariants of \mathbf{C}_e , and, as in [62, 114, 101], the parameters a_0 , a_1 , a_2 and a_3 are expressed in terms of Lamé’s parameters λ and μ , i.e.,

$$a_0 = \frac{2\mu + \lambda}{4a_3}, \quad a_1 = a_3 \frac{2\mu - \lambda}{2\mu + \lambda}, \quad a_2 = a_3 \frac{\lambda}{2\mu + \lambda}, \quad a_3 = a_1 + 2a_2 = 1. \quad (12)$$

Then, by using Equations (11a) and (11b), the constitutive part of the first Piola-Kirchhoff stress tensor reads [101]

$$\mathbf{P}_{sc} = J_\gamma \mathbf{F} \mathbf{F}_\gamma^{-1} \left(2 \frac{\partial \hat{\mathcal{W}}_\nu}{\partial \mathbf{C}_e}(\mathbf{C}_e) \right) \mathbf{F}_\gamma^{-T}. \quad (13)$$

Furthermore, we require the permeability tensor to be “*unconditionally isotropic*” [13], i.e., $\mathbf{k} = k_0 \mathbf{g}^{-1}$, so that the material permeability tensor reads

$$\mathbf{K} = J k_0 \mathbf{C}^{-1}. \quad (14)$$

In Equation (14), k_0 denotes the *scalar permeability* and is taken here as in [13, 62], i.e.,

$$k_0 = k_R \left[\frac{J - J_\gamma \Phi_{s\nu}}{J_\gamma \varphi_{fR}} \right]^{m_0} \exp \left(\frac{m_1}{2} \left[\frac{J^2 - J_\gamma^2}{J_\gamma^2} \right] \right), \quad (15)$$

where m_0 and m_1 are constant material coefficients, $\varphi_{fR} := 1 - \Phi_{s\nu}$ is a reference value of the fluid phase volumetric fraction, and k_R is the reference permeability of the medium. In the sequel, both k_R and φ_{fR} , and thus $\Phi_{s\nu}$, are assumed to be constant.

5 Constitutive Laws II: Non-Fickean diffusion

As pointed out in the Introduction, our aim is to generalise previous models of tumour growth [80, 101] by using some of the notions and tools offered by the theory of Fractional Calculus [92, 9, 12]. To this end, we introduce a non-Fickean type of diffusion of the chemical agents. Specifically, our purpose is to take into account the non-local behaviour of the gradient of the chemical agents’ mass fraction, and study its influence on the growth of an avascular tumour.

290 5.1 Non-Fickian mass flux vector

291 We propose to express the chemical species' mass flux vector, \mathbf{y}_α (see Equation (2c)), in terms
 292 of a non-local constitutive law of convolution type, in which, in the Euclidean case, the kernel
 293 of the convolution integral features a power law in the distance between the points x and \tilde{x}
 294 each pair (x, \tilde{x}) of spatial points occupied by body points. This way, we aim to show how \mathbf{y}_α ,
 295 evaluated at x , depends on the gradients of concentration evaluated at all other points \tilde{x} , and on
 296 the power law chosen for the convolution kernel. To do this, we face two difficulties: the first one
 297 is connected to the fact that, since, for the sake of generality, we view the body as a manifold, the
 298 concept of convolution has to be suitably generalised; the second one is due to the impossibility of
 299 integrating vector fields on manifolds. Whereas the first issue has been investigated in the literature
 300 [17, 106, 93], and we refer to the convolution on manifolds put forward in [106], the second issue
 301 can be circumvented by re-defining the mass flux vector of the chemical agents in weak form, i.e.,
 302 for each $t \in \mathcal{T}$, we define \mathbf{y}_α through the *duality* product [16]

$$\langle \mathbf{y}_\alpha, \text{grad } \check{c} \rangle := -\varrho_f \int_{\mathcal{B}_t} \left\{ \int_{\mathcal{B}_t} [\text{grad } \check{c}(x)] \mathbf{d}_\alpha(x, \tilde{x}, t) [\text{grad } c_\alpha(\tilde{x}, t)] \text{dv}(\tilde{x}) \right\} \text{dv}(x), \quad (16a)$$

$$\mathbf{d}_\alpha(x, \tilde{x}, t) := \mathfrak{f}_\alpha(x, \tilde{x}) \mathfrak{d}_\alpha(x, \tilde{x}, t), \quad (16b)$$

303 for all $\check{c} \in \check{\mathcal{C}} = \{\check{c} \in H^1(\mathcal{B}_t) : \check{c} = 0 \text{ on } (\partial\mathcal{B}_t)_D\}$, with $\check{\mathcal{C}}$ being the space of all *virtual variations*
 304 *of the mass fractions*, $(\partial\mathcal{B}_t)_D$ the portion of the boundary of \mathcal{B}_t on which Dirichlet conditions are
 305 applied for the mass fraction of the chemical agents, and $H^1(\mathcal{B}_t)$ is the standard Sobolev space of
 306 square-integrable functions over \mathcal{B}_t whose weak derivatives up to the order one are square-integrable
 307 over \mathcal{B}_t too.

308 We refer to the second-order tensor $\mathbf{d}_\alpha(x, \tilde{x}, t)$ as *non-local diffusivity tensor*, and we express
 309 it as the product of the scalar quantity $\mathfrak{f}_\alpha(x, \tilde{x})$ and of the tensor $\mathfrak{d}_\alpha(x, \tilde{x}, t)$. In particular, for a
 310 given $x \in \mathcal{B}_t$ and varying $\tilde{x} \in \mathcal{B}_t$, $\mathfrak{f}_\alpha(x, \tilde{x})$, referred to as the *non-locality function*, measures how
 311 the intensity of the chemical signal expressed by $\text{grad } c_\alpha(\tilde{x}, t)$ is felt at x . The tensor $\mathfrak{d}_\alpha(x, \tilde{x}, t)$,
 312 instead, is denominated *fractional diffusivity tensor*. We emphasise that \mathfrak{f}_α is defined for $x \neq \tilde{x}$
 313 and that, since we are dealing with fractional diffusion, both $\mathfrak{d}_\alpha(x, \tilde{x}, t)$ and $\mathbf{d}_\alpha(x, \tilde{x}, t)$ have, in
 314 general, physical dimensions different from those of the standard diffusivity tensor, depending on
 315 the prescription of \mathfrak{f}_α and $\alpha \in \mathbb{R}^+$.

316 The way in which $\mathfrak{f}_\alpha(x, \tilde{x})$ is to be understood in the case in which \mathcal{B}_t is viewed as a manifold
 317 is reported in Appendix A1. However, from here on, to avoid the technical difficulties of addressing
 318 such a general framework, which is out of the scope of this work, we prefer to adopt orthogonal
 319 Cartesian coordinates. Then, by regarding \mathcal{B}_t as a flat subset of \mathcal{S} having the same dimensionality
 320 as \mathcal{S} , $\mathfrak{f}_\alpha(x, \tilde{x})$ can be recast in the form $\mathfrak{f}_\alpha(x, \tilde{x}) = \hat{\mathfrak{f}}_\alpha(x - \tilde{x})$, where $\hat{\mathfrak{f}}_\alpha$ is introduced to re-define \mathfrak{f}_α as
 321 a function of the vector $x - \tilde{x}$, i.e., as $\hat{\mathfrak{f}}_\alpha : T_{\tilde{x}}\mathcal{S} \rightarrow \mathbb{R}$ (see Appendix A1). Furthermore, we require
 322 $\mathfrak{d}_\alpha(x, \tilde{x}, t)$ to be a two-point tensor of the type $\mathfrak{d}_\alpha(x, \tilde{x}, t) = \sum_{a,b=1}^3 [\mathfrak{d}_\alpha(x, \tilde{x}, t)]^{ab} \mathbf{e}_a(x) \otimes \mathbf{e}_b(\tilde{x})$,
 323 where $\{\mathbf{e}_l(x)\}_{l=1}^3$ and $\{\mathbf{e}_l(\tilde{x})\}_{l=1}^3$ are the vector bases attached to x and \tilde{x} . It is worth noticing
 324 that, within a Cartesian setting, and for $x = \tilde{x}$, the tensor $\mathbf{e}_a(x) \otimes \mathbf{e}_b(\tilde{x}) \equiv \mathbf{e}_a(x) \otimes \mathbf{e}_b(x)$ is referred
 325 to as "*Jacoby directional tensor*" in [3], where, in a slightly different context, the central Marchaud
 326 fractional derivative is extended to the case of two- or three-dimensional problems.

327 In general, there is no correlation at all between the vector bases $\{\mathbf{e}_l(x)\}_{l=1}^3$ and $\{\mathbf{e}_l(\tilde{x})\}_{l=1}^3$
 328 and, in fact, each basis can be chosen arbitrarily and independently of the other one. Nevertheless,
 329 $\{\mathbf{e}_l(\tilde{x})\}_{l=1}^3$ can be enforced to be the result of the parallel transport of $\{\mathbf{e}_l(x)\}_{l=1}^3$ along the geodesic

330 connecting x and \tilde{x} . In particular, in the Euclidean case, the arch of the geodesic connecting x and
331 \tilde{x} is the segment of the straight line directed from x to \tilde{x} and the parallel transport of $\{\mathbf{e}_l(x)\}_{l=1}^3$
332 along such a line renders $\{\mathbf{e}_l(\tilde{x})\}_{l=1}^3$ collinear with $\{\mathbf{e}_l(x)\}_{l=1}^3$. Hence, for each $l = 1, 2, 3$, $\mathbf{e}_l(x)$
333 and $\mathbf{e}_l(\tilde{x})$ can be associated with the same direction, hereafter denoted by \mathbf{i}_l , even though they
334 remain, implicitly, distinct vectors, attached to different spatial points. Within this approach, we
335 hypothesise that $\mathfrak{d}_\alpha(x, \tilde{x}, t)$ admits the representation $\mathfrak{d}_\alpha(x, \tilde{x}, t) = \sum_{b=1}^3 \mathfrak{d}_\alpha^b(x, \tilde{x}, t) \mathbf{e}_b(x) \otimes \mathbf{e}_b(\tilde{x})$
336 and, since $\mathbf{e}_l(x)$ is collinear with $\mathbf{e}_l(\tilde{x})$, this representation of $\mathfrak{d}_\alpha(x, \tilde{x}, t)$ mimics the description of
337 an orthotropic tensor function with respect to the set of directions $\{\mathbf{i}_1, \mathbf{i}_2, \mathbf{i}_3\}$. Hence, it is “as if”
338 we had $\mathfrak{d}_\alpha(x, \tilde{x}, t) = \sum_{b=1}^3 \mathfrak{d}_\alpha^b(x, \tilde{x}, t) \mathbf{i}_b \otimes \mathbf{i}_b$. Then, by using the definitions in Equation (16), we
339 identify the components of the fractional mass flux to be given by the following expression

$$[\mathbf{y}_\alpha(x, t)]^b := -\rho_f \int_{\mathcal{B}_t} \hat{\mathbf{f}}_\alpha(x - \tilde{x}) \mathfrak{d}_\alpha^b(x, \tilde{x}, t) \partial_b c_\alpha(\tilde{x}, t) \, \mathrm{d}v(\tilde{x}), \quad \text{no sum over } b = 1, 2, 3, \quad (17)$$

340 and we call the coefficients $\{\mathfrak{d}_\alpha^b(x, \tilde{x}, t)\}_{b=1}^3$ *fractional diffusivities*.

341 5.2 Comparison with other works

342 Other definitions of fractional mass flux vector can be found that characterise non-Fickian diffusion
343 processes (see e.g. [82, 105] and references therein). For instance, Sapora et al. [105] study a
344 fractional version of Darcy’s law in one dimension in which the filtration velocity (also known as
345 “specific mass flux”) is taken to be proportional to an integral operator that the Authors refer
346 to as “Riesz integral” [105] of pressure (note that the definition of Riesz integral given in [105]
347 differs by a factor $\cos(\beta\pi/2)$, with $\beta \in]0, 1[$, from that in [104, 9]). However, when passing to
348 higher dimensionalities, it is necessary to extend the concept of fractional differentiation to other
349 differential operators like the gradient of a scalar function. In this regard, in [40, 1, 113] the
350 fractional gradient of order $\alpha \in \mathbb{R}^+$ of a scalar function is defined as a co-vector, whose components
351 are identified with the fractional partial derivatives, each of which of order α , of the given function.
352 In particular, these fractional partial derivatives are taken in the sense of Riemann-Liouville in [40]
353 and in the sense of Caputo in [113], whereas the Nishimoto fractional derivative [87] is used in [1],
354 for $\alpha \in]0, 1]$.

355 For the purposes of our work, we adopt the definition given in Equation (17). This definition
356 presents some fundamental differences with respect to the definition supplied, for instance, in [105].
357 These differences, however, are not only related to the fact that the physical phenomenon addressed
358 in [105] is distinct from the one we are studying here. Rather, they are intrinsic in the definition
359 of the operator expressing \mathbf{y}_α , and can be summarised as follows:

- 360 • Equation (17) is conceived in a three-dimensional setting and, consequently, requires an
361 integration over the whole configuration of the body, \mathcal{B}_t , whereas the definition of the mass
362 flux given in [105] features an integration over a bounded interval.
- 363 • In our definition, each fractional diffusivity $\mathfrak{d}_\alpha^b(x, \tilde{x}, t)$, $b = 1, 2, 3$, is part of the integrand of
364 Equation (17), and cannot be factorised out of the corresponding integral.
- 365 • If, for a given $b_0 \in \{1, 2, 3\}$, the fractional diffusivity $\mathfrak{d}_\alpha^{b_0}(x, \tilde{x}, t)$ could be factorised out of
366 the integral in Equation (17) (e.g. by setting $\mathfrak{d}_\alpha^{b_0}(x, \tilde{x}, t) \equiv \mathfrak{d}_{0\alpha}$, with $\mathfrak{d}_{0\alpha}$ constant), and if

367 the only nonzero component of $\text{grad } c(\tilde{x}, t)$ were $\partial_{b_0} c_a(\tilde{x}, t)$ for all \tilde{x} and t , one would have

$$[\mathbf{y}_\alpha(x, t)]^{b_0} = -\varrho_f \mathfrak{D}_{0\alpha} \int_{\mathcal{B}_t} \hat{f}_\alpha(x - \tilde{x}) \partial_{b_0} c_a(\tilde{x}, t) dv(\tilde{x}), \quad (18)$$

368 where $\hat{f}_\alpha(x - \tilde{x})$ is still a function of *all* the components of the vector $x - \tilde{x}$, rather than of
 369 its b_0 -th component only. This property marks a major difference between our approach and
 370 the model developed in [105], and expresses the fact that, even in the presence of a preferred
 371 direction (i.e., the one associated with $\partial_{b_0} c_a$), one should account for the non-locality in all
 372 directions.

373 Before going further, we notice that, if the fractional diffusivities $\{\mathfrak{D}_\alpha^b(x, \tilde{x}, t)\}_{b=1}^3$ are all equal
 374 to some reference constant value $\mathfrak{D}_{R\alpha}$ (note that, for simplicity, we call ‘fractional diffusivities’ the
 375 *set of the three principal fractional diffusivities*), the mass flux vector $\mathbf{y}_\alpha(x, t)$ can be expressed (in
 376 a Cartesian setting) as

$$\mathbf{y}_\alpha(x, t) = -\varrho_f \mathfrak{D}_{R\alpha} \int_{\mathcal{B}_t} \hat{f}_\alpha(x - \tilde{x}) \text{grad } c_a(\tilde{x}, t) dv(\tilde{x}). \quad (19)$$

377 Moreover, for some suitable $\hat{f}_\alpha(x - \tilde{x})$, usually written as a power-law that decays in space, the
 378 integral on the right-hand-side of Equation (19) can be taken as the definition of a *fractional*
 379 *gradient* of c_a of order α , i.e., one can write (in the Cartesian setting)

$$\text{grad}^\alpha c_a(x, t) := \int_{\mathcal{B}_t} \hat{f}_\alpha(x - \tilde{x}) \text{grad } c_a(\tilde{x}, t) dv(\tilde{x}), \quad (20a)$$

$$[\text{grad}^\alpha c_a(x, t)]_b := \int_{\mathcal{B}_t} \hat{f}_\alpha(x - \tilde{x}) \partial_b c_a(\tilde{x}, t) dv(\tilde{x}), \quad b = 1, 2, 3. \quad (20b)$$

380 Equations (20a) and (20b) are reminiscent of the definition of fractional gradient of order α supplied
 381 in [113]. However, an important difference between that definition and ours is that, in [113], the
 382 components of the fractional gradient of c_a (i.e., $\{[\text{grad}^\alpha c_a(x, t)]_b\}_{b=1}^3$ in our notation) are identified
 383 with the Caputo derivatives of c_a along the principal directions of the vector basis. This, in turn,
 384 requires the function \hat{f}_α of Tarasov [113] to depend, for each Caputo derivative, solely on the b -th
 385 component of $x - \tilde{x}$.

386 5.3 Backward Piola transform of the mass flux vector

387 The backward Piola transformation of Equation (16a) is given by

$$\begin{aligned} \langle \mathbf{y}_\alpha, \text{grad} \check{c} \rangle &= \langle \mathbf{Y}_\alpha, \text{Grad} \check{c} \rangle \\ &= -\varrho_f \int_{\mathcal{B}} \left\{ \int_{\mathcal{B}} [\text{Grad} \check{c}(X, t)] \mathbf{D}_\alpha(X, \tilde{X}, t) [\text{Grad} \mathbf{c}_a(\tilde{X}, t)] dV(\tilde{X}) \right\} dV(X), \end{aligned} \quad (21)$$

388 with \check{c} and \mathbf{c}_a such that $\check{c}(X, t) = c(\chi(X, t))$ and $\mathbf{c}_a(X, t) = c_a(\chi(X, t), t)$, and we introduced the
 389 *material non-local diffusivity tensor*, \mathbf{D}_α , the *material non-locality function*, \mathfrak{F}_α , and the *material*
 390 *fractional diffusivity tensor*, \mathfrak{D}_α , as follows

$$\mathbf{D}_\alpha(X, \tilde{X}, t) := J(X, t) \mathfrak{F}_\alpha(X, \tilde{X}, t) \mathfrak{D}_\alpha(X, \tilde{X}, t), \quad (22a)$$

$$\mathfrak{F}_\alpha(X, \tilde{X}, t) := \hat{f}_\alpha(\chi(X, t) - \chi(\tilde{X}, t)), \quad (22b)$$

$$\mathfrak{D}_\alpha(X, \tilde{X}, t) := J(\tilde{X}, t) \mathbf{F}^{-1}(\chi(X, t), t) \mathfrak{d}_\alpha(\chi(X, t), \chi(\tilde{X}, t), t) \mathbf{F}^{-T}(\tilde{X}, t). \quad (22c)$$

391 More specifically, the components of $\mathfrak{D}_\alpha(X, \tilde{X}, t)$ and $\mathbf{Y}_\alpha(X, t)$ are given by

$$[\mathfrak{D}_\alpha(X, \tilde{X}, t)]^{AB} = J(\tilde{X}, t) \sum_{b=1}^3 [\mathbf{F}^{-1}(\chi(X, t), t)]^{A_b} \mathfrak{d}_\alpha^b(\chi(X, t), \chi(\tilde{X}, t), t) [\mathbf{F}^{-T}(\tilde{X}, t)]_b^B, \quad (23a)$$

$$[\mathbf{Y}_\alpha(X, t)]^A = -\varrho_f \int_{\mathcal{B}} J(X, t) \mathfrak{F}_\alpha(X, \tilde{X}, t) \sum_{B=1}^3 [\mathfrak{D}_\alpha(X, \tilde{X}, t)]^{AB} \partial_B \mathbf{c}_a(\tilde{X}, t) dV(\tilde{X}). \quad (23b)$$

392 Expression (23b) defines the components of the mass flux vector in the material description, whereas
 393 \mathfrak{D}_α is the material counterpart of the fractional diffusivity tensor \mathfrak{d}_α .

394 In the sequel, we assume the spatial fractional diffusivities to be all equal to each other, i.e.,
 395 $\mathfrak{d}_\alpha^b(x, \tilde{x}, t) = \mathfrak{d}_\alpha(x, \tilde{x}, t)$, for all $b = 1, 2, 3$, and that $\mathfrak{d}_\alpha(x, \tilde{x}, t)$ is independent of x (more rigorously,
 396 we should say that \mathfrak{d}_α can be redefined as a function of time and of the spatial variable with respect
 397 to which the integration is made, i.e., \tilde{x}). Consequently, with a slight abuse of notation, we simply
 398 write $\mathfrak{d}_\alpha(\tilde{x}, t)$. Moreover, following [101], we impose that $\mathfrak{d}_\alpha(\tilde{x}, t)$ depends on position and time
 399 through the volumetric fraction of the fluid phase, thereby setting $\mathfrak{d}_\alpha(\tilde{x}, t) = \varphi_f(\tilde{x}, t) \mathfrak{d}_{R\alpha}$, where
 400 $\mathfrak{d}_{R\alpha}$ is a *reference fractional diffusivity*, which is parameterised by α . Since $\varphi_f(\tilde{x}, t)$ can be related
 401 to the volumetric deformation of the solid phase and to growth through the expression (5b), we
 402 obtain

$$\mathfrak{d}_\alpha(\chi(\tilde{X}, t), t) = \frac{J(\tilde{X}, t) - J_\gamma(\tilde{X}, t) \Phi_{sv}}{J(\tilde{X}, t)} \mathfrak{d}_{R\alpha}. \quad (24)$$

403 These considerations imply that the components of \mathfrak{D}_α can be written as follows

$$[\mathfrak{D}_\alpha(X, \tilde{X}, t)]^{AB} = (J(\tilde{X}, t) - J_\gamma(\tilde{X}, t) \Phi_{sv}) \mathfrak{d}_{R\alpha} [\mathbf{F}^{-1}(\chi(X, t), t)]^{A_b} [\mathbf{F}^{-T}(\tilde{X}, t)]_b^B. \quad (25)$$

404 We notice that the non-local nature of the problem is also reflected in Equation (25). Indeed, in
 405 a model accounting only for local interactions, the last two terms of Equation (25) would give the
 406 inverse of the right Cauchy-Green deformation tensor \mathbf{C} , i.e., $\mathbf{C}^{-1} = \mathbf{F}^{-1} \cdot \mathbf{F}^{-T}$, since X and \tilde{X}
 407 would coincide. Still, this is not true in our case, since the non-locality changes with the dynamics
 408 of the tissue. Moreover, even in the case in which all the fractional diffusivities $\{\mathfrak{d}_\alpha^b(x, \tilde{x}, t)\}_{b=1}^3$
 409 were independent of x and \tilde{x} , their material counterparts $\{[\mathfrak{D}_\alpha(X, \tilde{X}, t)]^{AB}\}_{A,B=1}^3$ would still be
 410 functions of the points X and \tilde{X} because of the motion, χ .

411 **Remark 1** *Due to the non-local nature of the mass flux vector, its Piola transformation needs to*
 412 *be performed in two steps, i.e., as many as the integrals appearing in Equation (16a), or Equation*
 413 *(21). In particular, the volume ratio $J(X, t)$ is due to the change of measure of the outermost in-*
 414 *tegral of Equation (21), which re-defines the duality product between \mathbf{y}_α and $\text{grad}\check{c}$ into the duality*
 415 *product between \mathbf{Y}_α and $\text{Grad}\check{c}$. In our formalism, this volume ratio is used to define the pull-back*
 416 *of the non-local diffusivity tensor, \mathfrak{d}_α , as prescribed by Equations (22a)–(22c). Furthermore, the*
 417 *tensor $\mathbf{F}^{-1}(\chi(X, t), t)$ featuring in Equation (22c) stems from the transformation of the gradient*
 418 *of the virtual concentration, \check{c} , evaluated at x , i.e., $\text{grad}\check{c}(\chi(X, t), t) = \text{Grad}\check{c}(X, t) \mathbf{F}^{-1}(\chi(X, t), t)$,*

419 and it contributes, “from the left”, to the calculation of the pull-back of the fractional diffusivity
420 tensor. Whereas this first part of the backward Piola transformation of the mass flux vector is
421 standard, the second part of it reveals the non-locality of the constitutive law in Equation (21).
422 Indeed, the tensor $\mathbf{F}^{-\text{T}}(\tilde{X}, t)$ featuring in Equation (22c) must be evaluated in \tilde{X} because it origi-
423 nates from the transformation of the gradient of the concentration (not the virtual one), which is
424 part of the integrand of the innermost integral, i.e., the one expressing the non-local constitutive
425 law. This tensor contributes, “from the right”, to determine the pull-back of the fractional diffu-
426 sivity tensor. Finally, the volume ratio $J(\tilde{X}, t)$ is necessary because of the change of measure in
427 the innermost integral of Equation (16a) and is employed to define the pull-back of the fractional
428 diffusivity tensor, \mathfrak{D}_α . In conclusion, to determine the pull-back of the mass flux vector, a “double”
429 Piola transformation has to be performed.

430 **Remark 2** Looking at the Piola transformation of the mass flux vector, it is worth mentioning
431 that the non-locality of the problem, expressed through $\hat{\mathfrak{f}}_\alpha$ as a function of $(x - \tilde{x})$ in the current
432 configuration, cannot be described in general as a function of $(X - \tilde{X})$ in the reference configuration.
433 Rather, the material non-locality function, \mathfrak{F}_α , must be conceived as a function of the three variables
434 X , \tilde{X} and t since, as prescribed by Equation (22b), it inherits this dependence from the motion, χ ,
435 in a way that, in general, cannot be reduced to a function of time and of the difference $(X - \tilde{X})$.
436 Furthermore, we notice that the non-locality of the problem evolves from the reference to the current
437 configuration. Indeed, two points that are “close” in \mathcal{B} can either be “far away” from each other
438 or become “even closer” in \mathcal{B}_t , and vice versa.

439 6 Model summary and some numerical aspects

440 In this section, we summarise the equations characterising our mathematical model, specify the
441 expressions for the sinks and sources of mass, and highlight some computational aspects to be
442 taken into account. In the following, we focus on the case in which the considered chemical agents
443 are nutrient substances that are necessary to trigger and maintain the growth of the tumour. Hence,
444 we shall be referring to “nutrients” in lieu of “chemical agents” from here on.

445 6.1 Model equations

446 Our model is based on the following set of non-linear and coupled equations

$$\dot{\mathbf{c}}_{\text{p}} = [R_{\text{pn}} + R_{\text{fp}} - R_{\text{s}}\mathbf{c}_{\text{p}}][J_\gamma \Phi_{\text{s}\nu} \varrho_{\text{s}}]^{-1}, \quad (26\text{a})$$

$$\frac{\dot{\gamma}}{\gamma} = [R_{\text{fp}} + R_{\text{nf}}][3\varrho_{\text{s}} \Phi_{\text{s}\nu} J_\gamma]^{-1}, \quad (26\text{b})$$

$$\varrho_{\text{f}}[J - J_\gamma \Phi_{\text{s}\nu}]\dot{\mathbf{c}}_{\text{a}} - \varrho_{\text{f}}[\mathbf{K} \text{Grad} \mathbf{p}] \text{Grad} \mathbf{c}_{\text{a}} + \text{Div} \mathbf{Y}_\alpha = \mathbf{c}_{\text{a}} R_{\text{s}} + R_{\text{ap}}, \quad (26\text{c})$$

$$\dot{J} - \text{Div}(\mathbf{K} \text{Grad} \mathbf{p}) = 0, \quad (26\text{d})$$

$$\text{Div}(-J \mathbf{p} \mathbf{g}^{-1} \mathbf{F}^{-\text{T}} + \mathbf{P}_{\text{sc}}) = \mathbf{0}, \quad (26\text{e})$$

447 in the (4+3) unknowns $\mathcal{U} := \{\mathbf{c}_p, \gamma, \mathbf{c}_a, \mathbf{p}, \{\chi^a\}_{a=1}^3\}$, and with the source and sink terms [80, 101, 81]
 448

$$R_{\text{fp}} = J\zeta_{\text{fp}} \left\langle \frac{\mathbf{c}_a - \mathbf{c}_{\text{cr}}}{\mathbf{c}_{\text{env}} - \mathbf{c}_{\text{cr}}} \right\rangle_+ \left[1 - \frac{\delta_1 \langle \bar{\sigma} \rangle_+}{\delta_2 + \langle \bar{\sigma} \rangle_+} \right] \underbrace{\frac{J - J_\gamma \Phi_{\text{sv}}}{J \varphi_{\text{fR}}}}_{=\varphi_{\text{f}}/\varphi_{\text{fR}}} \underbrace{\frac{J_\gamma \Phi_{\text{sv}}}{J}}_{=\varphi_{\text{s}}} \mathbf{c}_p, \quad (27a)$$

$$R_{\text{nf}} = -J\zeta_{\text{nf}} \frac{J_\gamma \Phi_{\text{sv}}}{J} (1 - \mathbf{c}_p), \quad (27b)$$

$$R_{\text{ap}} = -J\zeta_{\text{ap}} \frac{\mathbf{c}_a}{\mathbf{c}_a + \mathbf{c}_0} \frac{J_\gamma \Phi_{\text{sv}}}{J} \mathbf{c}_p, \quad (27c)$$

$$R_{\text{pn}} = -J\zeta_{\text{pn}} \left\langle 1 - \frac{\mathbf{c}_a}{\mathbf{c}_{\text{cr}}} \right\rangle_+ \frac{J_\gamma \Phi_{\text{sv}}}{J} \mathbf{c}_p. \quad (27d)$$

449 In Equations (27a)–(27c), ζ_{fp} , ζ_{nf} , ζ_{ap} and ζ_{pn} are constants indicating the characteristic time
 450 scales with which the interstitial fluid is absorbed by the proliferating cells, the necrotic cells
 451 go into the fluid, nutrients are consumed, and proliferating cells die, respectively. The operator
 452 $\langle f \rangle_+ := \max\{0, f\}$ represents Macaulay’s brackets, which return the positive part of a function f .
 453 Moreover, \mathbf{c}_{cr} is a critical value for the nutrients’ mass fraction and \mathbf{c}_{env} refers to the concentration
 454 of nutrients present in the surrounding of the tumour. In order for growth to occur, it is necessary
 455 that $R_{\text{fp}} = Jr_{\text{fp}} > 0$, i.e., it must hold that $\mathbf{c}_a > \mathbf{c}_{\text{cr}}$, provided $\mathbf{c}_{\text{env}} > \mathbf{c}_{\text{cr}}$. We also mention that the
 456 mass source R_{fp} features the term in square brackets depending on $\bar{\sigma} := -\frac{1}{3} \text{tr} \boldsymbol{\sigma}$, which is introduced
 457 in order to describe the fact that growth can be modulated by mechanical stress, thereby giving rise
 458 to a phenomenon known as *mechanotransduction* [81, 80, 50, 56]. Finally, the product of the last
 459 three factors in Equation (27a) describes the fact that, to allow for the transfer of mass from the
 460 fluid to the proliferating cells, there must be a nonzero volumetric fraction of the fluid phase and
 461 of the solid phase as well as a nonzero mass fraction of the proliferating cells. Macaulay’s brackets
 462 in Equation (27d) ensure that the proliferating cells become necrotic, i.e., $R_{\text{pn}} < 0$ when $\mathbf{c}_a < \mathbf{c}_{\text{cr}}$,
 463 and $R_{\text{pn}} = 0$ otherwise. Equation (27b) assumes that R_{nf} is linear in the volumetric fraction of
 464 the solid phase and in the mass fraction of the necrotic cells, i.e., $1 - \mathbf{c}_p$, while R_{ap} establishes that
 465 the magnitude with which the nutrients are “eaten” by the proliferating cells depends on the ratio
 466 $\mathbf{c}_a/\mathbf{c}_0$, with $\mathbf{c}_0 \in]0, 1]$ being a reference value of the nutrients’ concentration that modulates their
 467 consumption. We refer the Reader to [81, 80, 101, 56] for further details on these terms, and for
 468 their generalisation to include growth-induced structural transformations.

469 Finally, we recall that the main goal of our model is to quantify the impact of the non-local
 470 diffusion of the nutrients, accounted for by \mathbf{Y}_α , on the overall evolution of the tumour, i.e., on all
 471 the unknowns of the model. We note that, apart from the presence of the fractional mass flux
 472 vector \mathbf{Y}_α , our model is the same as the one presented in [80] and extended in [101, 56].

473 6.2 Numerical aspects

474 The model summarised in Equation (26) features ordinary differential equations, partial differential
 475 equations and an integro-differential equation of fractional type. Since the model is formulated for
 476 a bounded domain and many couplings and nonlinearities are accounted for, the usual techniques
 477 adopted in Fractional Calculus for linear problems, such as the Fourier and Laplace transforms,
 478 cannot be used. Consequently, we need to resort to numerical techniques. In particular, we solve

479 Equations (26a)–(26e) by means of a FE scheme that we need to adapt to our purposes in order
 480 to take fractional derivatives into account. Here, we do not intend to go into the details of the
 481 numerical scheme, which is out of the scope of this work. Nevertheless, we intend to give some
 482 insights about the most important computational aspects of our work, while the numerical solutions
 483 are obtained by using COMSOL Multiphysics®.

484 Classical FE techniques [55, 103] have been used for solving numerically Equations (26a), (26b),
 485 (26d) and (26e), while Equation (26c) has required a special care. To this end, we report explicitly
 486 only the weak formulation corresponding to it. Before doing this, we denote with $(\partial\mathcal{B})_D$ and $(\partial\mathcal{B})_N$
 487 the Dirichlet and Neumann boundaries of \mathcal{B} , respectively, and assume $\partial\mathcal{B} = (\partial\mathcal{B})_D \sqcup (\partial\mathcal{B})_N$.
 488 Furthermore, by using the standard formalism for Sobolev spaces [16], and using the space of
 489 virtual concentrations, $\tilde{\mathcal{C}}_R := \{\tilde{\mathbf{c}} \in H^1(\mathcal{B}) \text{ s.t. } \tilde{\mathbf{c}}|_{(\partial\mathcal{B})_D} = 0\}$, we have that, for all $\tilde{\mathbf{c}} \in \tilde{\mathcal{C}}_R$, the
 490 following weak form applies

$$\begin{aligned} & \int_{\mathcal{B}} \{\varrho_f[J - J_\gamma \Phi_{sv}] \dot{\mathbf{c}}_a - \varrho_f[\mathbf{K} \text{Grad} \mathbf{p}] \text{Grad} \mathbf{c}_a - \mathbf{c}_a R_s - R_{ap}\} \tilde{\mathbf{c}} \, dV \\ & - \int_{\mathcal{B}} \mathbf{Y}_\alpha \text{Grad} \tilde{\mathbf{c}} \, dV + \int_{(\partial\mathcal{B})_N} \mathbf{Y}_\alpha \cdot \mathbf{N} \tilde{\mathbf{c}} \, dS = 0, \end{aligned} \quad (28)$$

491 where \mathbf{N} is the field of unit vectors normal to $(\partial\mathcal{B})_N$ while \mathbf{Y}_α is given in Equation (21), so that
 492 the second volume integral of Equation (28) (without the sign) becomes

$$\begin{aligned} & \int_{\mathcal{B}} \mathbf{Y}_\alpha(X, t) \text{Grad} \tilde{\mathbf{c}}(X, t) \, dV(X) \\ & = -\varrho_f \int_{\mathcal{B}} \left\{ \int_{\mathcal{B}} [\text{Grad} \tilde{\mathbf{c}}(X, t)] \mathbf{D}_\alpha(X, \tilde{X}, t) [\text{Grad} \mathbf{c}_a(\tilde{X}, t)] \, dV(\tilde{X}) \right\} \, dV(X). \end{aligned} \quad (29)$$

493 After applying a backward Euler scheme for the time derivative, a linearisation procedure, and
 494 Galerkin method, Equation (28) leads to a system of algebraic equations that, except for a *non-local*
 495 *stiffness matrix*, arising from the double integral in Equation (29), is similar to the one obtained in
 496 standard FE approaches. From a numerical point of view, the non-local stiffness matrix reflects a
 497 long range coupling among the elements in the spatial discretisation. Indeed, it is worth noting that,
 498 in the construction of the non-local stiffness matrix, the cross integrations between the piecewise
 499 polynomial *ansatz* functions do not vanish as they would in the case of the stiffness matrix of
 500 a standard diffusion problem. That is, even though two discretisation nodes are far away from
 501 each other, the entry of the matrix corresponding to these nodes will be non-zero, because of the
 502 presence of the non-locality function \hat{f}_α . This results into stiffness matrices that are denser, the
 503 stronger the non-locality is. In fact, this is a typical feature of the numerical study of non-local
 504 differential equations based on the use of FE methods (see for instance [47]). Still, as pointed out
 505 in [47], standard techniques for the solution of such equations, like Gauss elimination, can be used.

506 Before closing this section, we would like to remark that, in the simulations carried out in our
 507 work, the stiffness matrix associated with Equation (29) is symmetric and positive definite.

508 7 Benchmark problem and considerations on the non- 509 locality function

510 In this section, we specify a benchmark problem in order to simplify and solve the mathematical
511 model given by Equations (26a)-(26e). To this end, we make use of the problem proposed in [5],
512 and recently investigated in [101, 56] to account for growth-induced inelastic distortions. By doing
513 this, we intend to model the volumetric growth of an avascular tumour in a “jacketed” cylindrical
514 sample (its deformation is restricted to be along the longitudinal axis only), and to investigate, how
515 and to what extent, the non-local diffusivity properties of the nutrients influence the dynamics of
516 the tissue. In the following, we assume that the problem complies with axial symmetry and that
517 it is radially homogeneous regardless of how slender the cylindrical sample is. This will require
518 suitable *a priori* restrictions on all the unknowns of the problem.

519 7.1 Description of the benchmark problem

520 As in [101, 56], we adopt the cylindrical coordinates (R, Θ, Z) and (r, ϑ, z) , associated with the
521 reference and the current configurations of the tumour, respectively. Moreover, we require the
522 motion to satisfy with the conditions

$$\chi^r(R, \Theta, Z, t) = r = R, \quad (30a)$$

$$\chi^\vartheta(R, \Theta, Z, t) = \vartheta = \Theta, \quad (30b)$$

$$\chi^z(R, \Theta, Z, t) = z = Z + u(Z, t), \quad (30c)$$

523 where u is the unknown axial component of displacement. In this situation, the tumour is allowed
524 to expand itself solely along the axial direction and χ^z is the only unknown component of the
525 motion, χ . Additionally, to comply with the axial symmetry and with the radial homogeneity of
526 the problem, the pressure \mathbf{p} is considered to be a function of the axial coordinate and time only.
527 Another restriction pertains to the growth parameter γ , which is also assumed to depend only on
528 Z and t (note that since the growth tensor $\mathbf{F}_\gamma = \gamma \mathbf{I}$ is spherical, it maintains the symmetries of
529 the problem). Similar requirements also apply for the mass fraction of the proliferating cells, \mathbf{c}_p ,
530 as well as for the mass fraction of the nutrients, \mathbf{c}_a .

531 The motion we have assumed implies that the matrix representations of the deformation gra-
532 dient tensor \mathbf{F} and of the right Cauchy-Green deformation tensor \mathbf{C} read

$$[\mathbf{F}] = \text{diag}\{1, 1, 1 + u'\}, \quad (31a)$$

$$[\mathbf{C}] = \text{diag}\{1, 1, [1 + u']^2\}, \quad (31b)$$

533 where u' denotes the derivative of u in the axial direction. Since it holds that $J = \det(\mathbf{F}) = 1 + u' >$
534 0 , u' must obey the inequality $u' > -1$.

535 Additionally, the growth tensor admits the diagonal form

$$[\mathbf{F}_\gamma] = \text{diag}\{\gamma, \gamma, \gamma\}, \quad \gamma > 0, \quad (32)$$

536 and, consequently, the elastic right Cauchy-Green deformation tensor \mathbf{C}_e has the representation

$$[\mathbf{C}_e] = \text{diag} \left\{ \frac{1}{\gamma^2}, \frac{1}{\gamma^2}, \frac{[1 + u']^2}{\gamma^2} \right\}. \quad (33)$$

537 Because of Equations (31a), (31b), (32) and (33), of the symmetry properties of the pressure
 538 term $-J\mathbf{p}\mathbf{g}^{-1}\mathbf{F}^{-\text{T}}$, and of the constitutive expression (13), the first Piola-Kirchhoff stress tensor
 539 $\mathbf{P} = -J\mathbf{p}\mathbf{g}^{-1}\mathbf{F}^{-\text{T}} + \mathbf{P}_{\text{sc}}$ has the diagonal representation

$$[\mathbf{P}] = \text{diag} \left\{ -J\mathbf{p} + [\mathbf{P}_{\text{sc}}]^{rR}, -J\mathbf{p} + [\mathbf{P}_{\text{sc}}]^{\vartheta\Theta}, -\mathbf{p} + [\mathbf{P}_{\text{sc}}]^{zZ} \right\}, \quad (34)$$

540 where each quantity featuring in each component of \mathbf{P} is a function solely of Z and time. Moreover,
 541 it applies that $[\mathbf{P}_{\text{sc}}]^{rR} = [\mathbf{P}_{\text{sc}}]^{\vartheta\Theta}$ and, thus, the balance of linear momentum (26e) in cylindrical
 542 coordinates reduces to

$$\frac{\partial}{\partial Z} (-\mathbf{p} + [\mathbf{P}_{\text{sc}}]^{zZ}) = 0. \quad (35)$$

543 This result can be found also in other benchmark problems, such as the confined compression
 544 tests of articular cartilage, under symmetry assumptions similar to those made here. Therefore,
 545 Equation (35) constitutes a simplification obtained by virtue of symmetry and not by invoking the
 546 slenderness of the cylinder used in our benchmark (see Table 1).

547 Note also that, according to Equations (14) and (15), the conditions imposed on the deformation
 548 and on the growth tensor are such that k_0 depends, through J and J_γ , only on the axial coordinate
 549 and on time. Moreover, the same conclusion can be drawn for the diffusivity \mathfrak{d}_α , which, with slight
 550 abuse of notation, we express as $\mathfrak{d}_\alpha(Z, t)$ from here on.

551 By following the same reasoning that has led to Equation (35), and noticing that the only
 552 non-zero component of the mass flux \mathbf{Q} is the axial one, i.e., $\mathbf{Q}^Z = -\mathbf{K}^{ZZ} \frac{\partial \mathbf{p}}{\partial Z}$ with $\mathbf{K}^{ZZ} =$
 553 $Jk_0[\mathbf{C}^{-1}]^{ZZ} = k_0/(1 + u')$, the continuity equation (26d) becomes

$$\frac{\partial^2 u}{\partial Z \partial t} - \frac{\partial}{\partial Z} \left(\frac{k_0}{1 + u'} \frac{\partial \mathbf{p}}{\partial Z} \right) = 0. \quad (36)$$

554 The equations for \mathbf{c}_p and γ , that is Equations (26a) and (26b), are scalar ODEs, and the fact
 555 that \mathbf{c}_p and γ depend only of Z and t is consistent with the symmetry properties of all the terms
 556 featuring in these equations. That said, a remark is in order for Equation (26b) to emphasise that
 557 the considered benchmark problem remains three-dimensional in spite of the axial symmetry and
 558 radial homogeneity that it enjoys. Indeed, looking at the source R_{fp} in Equation (27a), we notice
 559 that the mechanotransduction term (i.e., the term between brackets in Equation (27a)) features
 560 the trace of Cauchy stress tensor, which requires the evaluation of all the stress components, i.e.,
 561 also of those in the radial and circumferential directions, these being non null because the cylinder
 562 is laterally jacketed. Therefore, we conclude that, even though the cylinder used for our benchmark
 563 problem is slender, with slenderness ratio $2 \cdot 10^{-2}$ (see the geometric data in Table 1), the problem
 564 itself necessitates to account for all the geometrical dimensions.

565 The last equation to consider is the balance law for \mathbf{c}_a (see Equation (26c)) in which the
 566 non-standard mass flux \mathbf{Y}_α features, at least in principle, all the coordinates (i.e., also the radial
 567 and the circumferential coordinates) through the non-locality function $\mathfrak{F}_\alpha(X, \tilde{X}, t) = \hat{\mathfrak{f}}_\alpha(\chi(X, t) -$
 568 $\chi(\tilde{X}, t))$. To maintain the axial symmetry of the problem and to eliminate the dependence of
 569 the nutrients' mass flux on the radial and circumferential coordinates, two paths may be followed.
 570 One is discussed in Section "Definition of the non-locality function" and, for consistency with the
 571 symmetry requirements introduced so far, it imposes to rephrase the non-locality function as a
 572 function of the axial coordinate only. However, another path —valid for the problem at hand—

573 could be to eliminate the dependence of the non-locality function on the radial and circumferential
574 coordinate by taking advantage of the slenderness of the cylinder. To this end, we write the non-
575 locality function as

$$\hat{f}_\alpha(x - \tilde{x}) = f_{0\alpha} \frac{1}{\|x - \tilde{x}\|^\alpha} = f_{0\alpha} \frac{1}{\|(z - \tilde{z})\mathbf{e}_z + \mathbf{r}_t\|^\alpha}, \quad (37)$$

576 where \mathbf{e}_z is the unit vector along which the cylinder's axis is directed, $f_{0\alpha}$, with $\alpha \in]0, 1[$, is an
577 α -dependent coefficient to be individuated, and \mathbf{r}_t is a vector lying on the cross-section of the
578 cylinder. Next, we rescale the axial vector $(z - \tilde{z})\mathbf{e}_z$ by the undeformed length of the cylinder, i.e.,
579 $2L_{\text{in}}$, and the transverse vector \mathbf{r}_t by the cylinder diameter prior to deformation, i.e., $2R_{\text{in}}$, so that
580 Equation (37) becomes

$$\hat{f}_\alpha(x - \tilde{x}) = f_{0\alpha} \frac{1}{\|2L_{\text{in}}\boldsymbol{\rho}_a + 2R_{\text{in}}\boldsymbol{\rho}_t\|^\alpha} = \frac{f_{0\alpha}}{(2L_{\text{in}})^\alpha} \frac{1}{\|\boldsymbol{\rho}_a + (R_{\text{in}}/L_{\text{in}})\boldsymbol{\rho}_t\|^\alpha}, \quad (38)$$

581 with $\boldsymbol{\rho}_a = (z - \tilde{z})\mathbf{e}_z / (2L_{\text{in}})$ and $\boldsymbol{\rho}_t := \mathbf{r}_t / (2R_{\text{in}})$. Now, since the slenderness ratio $R_{\text{in}}/L_{\text{in}}$ is $2 \cdot 10^{-2}$,
582 we assume, within the first approximation, that the non-locality function can be truncated at the
583 zero-th order in the slenderness ratio, thereby taking the expression

$$\hat{f}_\alpha(x - \tilde{x}) \approx \frac{f_{0\alpha}}{(2L_{\text{in}})^\alpha} \frac{1}{\|\boldsymbol{\rho}_a\|^\alpha} = f_{0\alpha} \frac{1}{\|(z - \tilde{z})\mathbf{e}_z\|^\alpha} = f_{0\alpha} \frac{1}{|z - \tilde{z}|^\alpha}. \quad (39)$$

584 As discussed below, the coefficient $f_{0\alpha}$ acquires the meaning of a normalisation factor.

585 7.2 Initial and boundary conditions

586 To solve Equations (26a)–(26e), we impose the same boundary and initial conditions used in
587 [101, 56]. Specifically, at the initial instant of time we consider a reference configuration being
588 characterised by the following relations

$$\chi^r(R, \Theta, Z, 0) = R, \quad \chi^\theta(R, \Theta, Z, 0) = \Theta, \quad \chi^z(R, \Theta, Z, 0) = Z, \quad (40)$$

589 where $R \in [0, R_{\text{in}}[$, $\Theta \in [0, 2\pi[$ and $Z \in [-L_{\text{in}}, +L_{\text{in}}]$, while R_{in} and $2L_{\text{in}}$ denote the radius and
590 the length of the undeformed specimen. Besides, we enforce that, at $t = 0$, necrotic cells are
591 absent, i.e., $\mathbf{c}_p(R, \Theta, Z, 0) = 1$, the fluid pressure is zero, i.e., $\mathbf{p}(R, \Theta, Z, 0) = 0$, the nutrients' mass
592 fraction equals the environmental one, i.e., $\mathbf{c}_a(R, \Theta, Z, 0) = \mathbf{c}_{\text{env}} > 0$, and the distribution of the
593 growth parameter is homogeneous and unitary, i.e., $\gamma(R, \Theta, Z, 0) = 1$. In addition, we consider the
594 following boundary conditions

$$(-J\mathbf{p}\mathbf{g}^{-1}\mathbf{F}^{-\text{T}} + \mathbf{P}_{\text{sc}}) \cdot \mathbf{N}_A = \mathbf{0}, \quad \text{on } (\partial\mathcal{B})_{\text{Left}} \text{ and } (\partial\mathcal{B})_{\text{Right}}, \quad (41a)$$

$$(-\mathbf{K}\text{Grad}\mathbf{p}) \cdot \mathbf{N}_C = 0, \quad \text{on } (\partial\mathcal{B})_C, \quad (41b)$$

$$\mathbf{p} = 0, \quad \text{on } (\partial\mathcal{B})_{\text{Left}} \text{ and } (\partial\mathcal{B})_{\text{Right}}, \quad (41c)$$

$$\mathbf{c}_a = \mathbf{c}_{\text{env}}, \quad \text{on } (\partial\mathcal{B})_{\text{Left}} \text{ and } (\partial\mathcal{B})_{\text{Right}}, \quad (41d)$$

$$\mathbf{Y}_\alpha \cdot \mathbf{N}_C = 0, \quad \text{on } (\partial\mathcal{B})_C, \quad (41e)$$

595 where \mathbf{N}_A and \mathbf{N}_C are fields of unit vectors normal to $(\partial\mathcal{B})_{\text{Left}} \cup (\partial\mathcal{B})_{\text{Right}}$ and to $(\partial\mathcal{B})_C$, respec-
596 tively, and $\partial\mathcal{B} = (\partial\mathcal{B})_{\text{Left}} \cup (\partial\mathcal{B})_{\text{Right}} \cup (\partial\mathcal{B})_C$. Specifically, $(\partial\mathcal{B})_{\text{Left}}$ and $(\partial\mathcal{B})_{\text{Right}}$ are the left
597 and the right surfaces at the extremities of \mathcal{B} , and $(\partial\mathcal{B})_C$ is the lateral boundary.

598 7.3 Definition of the non-locality function

599 A classical approach for defining \hat{f}_α is to adopt a power-law that decays in space. To our knowledge,
600 this is customary for problems that are *a priori* formulated as one-dimensional and in which $\hat{f}_\alpha(x-\tilde{x})$
601 is assumed to be proportional to the reciprocal of $|x-\tilde{x}|^\alpha$, with x and \tilde{x} being points of the real
602 line or of an interval of finite length [112, 11, 108, 22, 105]. This choice permits to “import”,
603 with slight modifications, the definitions of the fractional derivatives in time (see e.g. [9]) to the
604 fractional differentiation in space. However, in some situations it is necessary to assess an *a priori*
605 relationship between the dimensionality of the problem under study and the non-locality that *must*
606 —or *may*— be resolved, once the dimensionality has been settled. Indeed, in a three-dimensional
607 problem endowed with the symmetry and homogeneity properties we are dealing with, the only
608 non-zero partial derivative of the concentration is the one along the axial direction. In such a
609 situation, the axial mass flux reads

$$[\mathbf{y}_\alpha(x, t)]^z = -\varrho_f \int_{\mathcal{B}_t} \hat{f}_\alpha(x - \tilde{x}) \mathfrak{d}_\alpha(\tilde{z}, t) \partial_{\tilde{z}} c_a(\tilde{z}, t) \, \text{d}v(\tilde{x}), \quad (42)$$

610 whereas the radial and the circumferential components of the flux are zero. Note that we are using
611 here the customary formalism for cylindrical coordinates, so that $\tilde{x} = (\tilde{r}, \tilde{\vartheta}, \tilde{z})$. As anticipated
612 before, the expression for $[\mathbf{y}_\alpha(x, t)]^z$ reminds the definition of fractional gradient given in [113],
613 with the difference that a volume integral is used in (42) and that all the components of $x - \tilde{x}$ are
614 considered.

615 In spite of the fact that the problem is one-dimensional from the point of view of its symmetries,
616 the axial flux is still determined by an integration over the three-dimensional region \mathcal{B}_t , and $\hat{f}_\alpha(x-\tilde{x})$
617 describes, as it stands, a non-locality in three dimensions (trivially, because $x - \tilde{x}$ is a vector of
618 a three-dimensional vector space). Therefore, the component of $(x - \tilde{x})$ along the radial or the
619 circumferential direction will influence the axial mass flux, even though the problem was claimed
620 to enjoy axial symmetry and to be independent of the radial coordinate. This result, however, may
621 be physically unsound. Indeed, one would expect non-locality to be coherent with the symmetries
622 of the problem, even though the integral of Equation (42) is over the whole configuration \mathcal{B}_t ,
623 thereby maintaining the physical dimensionality of the problem itself.

624 To address this issue, we need to take into account how the symmetries of the problem under
625 investigation influence the non-locality in the relationship between \mathbf{y}_α and c_a . Consequently, the
626 non-locality function \hat{f}_α in Equation (42) is re-defined as

$$\hat{f}_\alpha(x - \tilde{x}) := \hat{h}_\alpha(z - \tilde{z}) = \frac{1}{\mathcal{N}(\alpha)} \frac{1}{|z - \tilde{z}|^\alpha}, \quad \alpha \in]0, 1[, \quad (43)$$

627 where $\mathcal{N}(\alpha)$ is a normalisation factor to be determined. From Equations (42) and (43), we notice
628 that the physical dimensions of the fractional diffusivity, \mathfrak{d}_α , are $L^{1+\alpha}T^{-1}$, where L and T stand
629 for the characteristic “length” and the characteristic “time” of the non-local diffusion process,
630 respectively. Thus, when α tends to 1 (from below), we recover the physical dimensions of the
631 standard diffusivity.

632 By substituting Equation (43) into Equation (42), and recalling that $\mathcal{B}_t = \mathcal{C}_R \times]-\ell(t), +\ell(t)[$
633 (where \mathcal{C}_R is the cross-section of the cylinder and $2\ell(t)$ is its variable axial length), we obtain the
634 much simpler expression

$$[\mathbf{y}_\alpha(x, t)]^z \equiv y_\alpha^z(z, t) = -\frac{\varrho_f \pi R_{\text{in}}^2}{\mathcal{N}(\alpha)} \int_{-\ell(t)}^{+\ell(t)} \frac{1}{|z - \tilde{z}|^\alpha} \mathfrak{d}_\alpha(\tilde{z}, t) \partial_{\tilde{z}} c_a(\tilde{z}, t) \, \text{d}\tilde{z}. \quad (44)$$

635 For the Equation (44) to be physically sound, it has to return the axial component of the standard
636 mass flux vector in the limit $\alpha \rightarrow 1^-$. Unfortunately, proving this result for problems defined over
637 bounded domains is not possible without knowing c_a . On the contrary, this difficulty does not arise
638 in problems defined over unbounded domains, because, with the aid of the Fourier transform, it is
639 possible to do the following reasoning:

- 640 • Introduce the auxiliary notation $\psi_\alpha^z(\tilde{z}, t) := -\varrho_f \mathfrak{d}_\alpha(\tilde{z}, t) \partial_z c_a(\tilde{z}, t)$, and assume to prolong
641 $y_\alpha^z(z, t)$ to the whole real line, so that Equation (44) becomes

$$\begin{aligned} y_\alpha^z(z, t) &= -\frac{\varrho_f \pi R_{\text{in}}^2}{\mathcal{N}(\alpha)} \int_{-\infty}^{+\infty} \frac{1}{|z - \tilde{z}|^\alpha} \mathfrak{d}_\alpha(\tilde{z}, t) \partial_z c_a(\tilde{z}, t) d\tilde{z} \\ &= \pi R_{\text{in}}^2 \int_{-\infty}^{+\infty} \hat{\mathfrak{h}}_\alpha(z - \tilde{z}) \psi_\alpha^z(\tilde{z}, t) d\tilde{z} \\ &= \pi R_{\text{in}}^2 [\hat{\mathfrak{h}}_\alpha * \psi_\alpha^z(\cdot, t)](z), \end{aligned} \quad (45)$$

642 thereby expressing $y_\alpha^z(z, t)$ as the convolution product between $\hat{\mathfrak{h}}_\alpha$ and $\psi_\alpha^z(\cdot, t)$.

- 643 • Compute the Fourier transform of $y_\alpha^z(z, t)$ as written in Equation (45), i.e.,

$$\begin{aligned} \mathcal{F}[y_\alpha^z(\cdot, t)](\xi) &:= \int_{-\infty}^{+\infty} y_\alpha^z(z, t) \exp(-i\xi z) dz \\ &= \pi R_{\text{in}}^2 \mathcal{F}[\hat{\mathfrak{h}}_\alpha](\xi) \mathcal{F}[\psi_\alpha^z(\cdot, t)](\xi) \\ &= \pi R_{\text{in}}^2 \frac{2\Gamma(1 - \alpha)}{\mathcal{N}(\alpha)} \sin\left(\frac{\alpha\pi}{2}\right) |\xi|^{\alpha-1} \mathcal{F}[\psi_\alpha^z(\cdot, t)](\xi), \end{aligned} \quad (46)$$

644 where $\xi \in \mathbb{R} \setminus \{0\}$ is the wave number, $\Gamma(\cdot)$ is the Euler Gamma function and we used the
645 Fourier transform of $\hat{\mathfrak{h}}_\alpha$, i.e.,

$$\mathcal{F}[\hat{\mathfrak{h}}_\alpha](\xi) = \frac{2\Gamma(1 - \alpha)}{\mathcal{N}(\alpha)} \sin\left(\frac{\alpha\pi}{2}\right) |\xi|^{\alpha-1}. \quad (47)$$

646 Since $\mathcal{F}[y_\alpha^z(\cdot, t)](\xi)$ is proportional to the product of $\mathcal{F}[\hat{\mathfrak{h}}_\alpha](\xi)$ and $\mathcal{F}[\psi_\alpha^z(\cdot, t)](\xi)$, one can
647 identify the non-local contribution of the mass flux with $\mathcal{F}[\hat{\mathfrak{h}}_\alpha](\xi)$, given in Equation (47).

648 Note that, if $\mathfrak{d}_\alpha(z, t)$ and $c_a(z, t)$ are both assumed to be even with respect to $z = 0$ —an
649 assumption that is consistent with the hypothesis, done later, that the considered problem
650 is symmetric with respect to $z = 0$ —, $\mathcal{F}[y_\alpha^z(\cdot, t)](\xi)$ can be prolonged to $\xi = 0$ and is null for
651 this value. To see this, we first rewrite $\mathcal{F}[\psi_\alpha^z(\cdot, t)](\xi)$ as

$$\mathcal{F}[\psi_\alpha^z(\cdot, t)](\xi) = -\varrho_f \int_{-\infty}^{+\infty} \mathfrak{d}_\alpha(z, t) \partial_z c_a(z, t) \exp(-i\xi z) dz. \quad (48)$$

652 Then, we notice that $\mathcal{F}[\psi_\alpha^z(\cdot, t)](0)$ is zero, because $\mathfrak{d}_\alpha(z, t)$ is even and $\partial_z c_a(z, t)$ is odd
653 with respect to $z = 0$ for all times. Moreover, because of this result, it also holds that
654 $\lim_{\xi \rightarrow 0} |\xi|^{\alpha-1} \mathcal{F}[\psi_\alpha^z(\cdot, t)](\xi) = 0$, and, consequently, $\lim_{\xi \rightarrow 0} \mathcal{F}[y_\alpha^z(\cdot, t)](\xi) = 0$ too.

655 • Compute the limit of $\mathcal{F}[y_\alpha^z(\cdot, t)](\xi)$ for $\alpha \rightarrow 1^-$, and find $\mathcal{N}(\alpha)$ such that

$$\begin{aligned} \lim_{\alpha \rightarrow 1^-} \mathcal{F}[y_\alpha^z(\cdot, t)](\xi) &= \lim_{\alpha \rightarrow 1^-} \mathcal{F}[\psi_\alpha^z(\cdot, t)](\xi) \\ &= \mathcal{F}[-\varrho_f \mathfrak{d}_1(\cdot, t) \partial_z c_a(\cdot, t)](\xi), \end{aligned} \quad (49)$$

656 with $\mathfrak{d}_1(\tilde{z}, t) := \lim_{\alpha \rightarrow 1^-} \mathfrak{d}_\alpha(\tilde{z}, t)$. We emphasise that this limit is taken uniformly with respect
657 to the pairs (\tilde{z}, t) and, in particular, looking at Equation (24), it turns out to be uniform
658 with respect to the motion, so that it is intended as

$$\begin{aligned} \lim_{\alpha \rightarrow 1^-} \mathfrak{d}_\alpha(\tilde{z}, t) &= \lim_{\alpha \rightarrow 1^-} \mathfrak{d}_\alpha(\chi^z(\tilde{X}, t), t) = \frac{J(\tilde{X}, t) - J_\gamma(\tilde{X}, t)\Phi_{s\nu}}{J(\tilde{X}, t)} \lim_{\alpha \rightarrow 1^-} \mathfrak{d}_{R\alpha} \\ &= \frac{J(\tilde{X}, t) - J_\gamma(\tilde{X}, t)\Phi_{s\nu}}{J(\tilde{X}, t)} \mathfrak{d}_{R1}, \end{aligned} \quad (50)$$

659 where, in our model, \mathfrak{d}_{R1} is a constant having the physical dimensions of a standard diffusivity
660 coefficient. In particular, to meet this requirement, we choose $\mathfrak{d}_{R\alpha}$ as

$$\mathfrak{d}_{R\alpha} := d_R L^{\alpha-1}, \quad (51)$$

661 with d_R being a constant reference value for the standard diffusivity coefficient [13], so that
662 $\mathfrak{d}_{R1} = d_R$.

663 One possible way to comply with Equation (49) is that $\mathcal{N}(\alpha)$ satisfies the relation

$$\lim_{\alpha \rightarrow 1^-} \frac{2\Gamma(1-\alpha)\pi R_{\text{in}}^2}{\mathcal{N}(\alpha)} = 1. \quad (52)$$

664 Then, for Equation (44) to be (up to the diffusivity \mathfrak{d}_α) Caputo's symmetrised fractional derivative
665 of the mass fraction, c_a , which is defined over the interval $] -\ell(t), +\ell(t)[$, we choose the stronger
666 condition

$$\mathcal{N}(\alpha) = 2\Gamma(1-\alpha)\pi R_{\text{in}}^2, \quad \alpha \in]0, 1[. \quad (53)$$

667 Clearly, Equation (53) represents a “guess”, because we are unable to compute directly the nor-
668 malisation factor for a bounded interval. Nevertheless, plugging Equation (53) into Equation (44)
669 yields

$$y_\alpha^z(z, t) = -\frac{\varrho_f}{2\Gamma(1-\alpha)} \int_{-\ell(t)}^{+\ell(t)} \frac{1}{|z - \tilde{z}|^\alpha} \mathfrak{d}_\alpha(\tilde{z}, t) \partial_{\tilde{z}} c_a(\tilde{z}, t) d\tilde{z}, \quad (54)$$

670 which, apart from the spatial dependence of the fractional diffusivity $\mathfrak{d}_\alpha(\tilde{z}, t)$, coincides with the
671 definition of fractional mass flux in one dimension used by other Authors, see for instance [89, 35]
672 and the references therein. Furthermore, in the case in which the fractional diffusivity can be
673 factorised outside the integral operator, e.g. by setting $\mathfrak{d}_\alpha(\tilde{z}, t) = \mathfrak{d}_{0\alpha}$, the axial mass flux becomes
674 proportional to the symmetrised Caputo fractional derivative of order α of c_a [9].

675 **Remark 3 ((On the normalisation factor))** We notice that, apart from the presence of the
676 area of the cylinder's cross-section $|\mathcal{C}_R| = \pi R_{\text{in}}^2$, the expression of the normalisation factor $\mathcal{N}(\alpha)$
677 given in Equation (53) coincides with the one used in other works (see e.g. [112, 11, 22]). Never-
678 theless, by looking at Equation (46), one can see that other definitions of the normalisation factor
679 can be employed which satisfy the condition of Equation (49). Indeed, if the limit in Equation (52)
680 is rephrased as

$$\lim_{\alpha \rightarrow 1^-} \frac{2\Gamma(1-\alpha) \sin(\alpha\pi/2) \pi R_{\text{in}}^2}{\hat{\mathcal{N}}(\alpha)} = 1, \quad (55)$$

681 where $\hat{\mathcal{N}}(\alpha)$ is the new normalisation factor sought for, then, upon following the reasoning leading
682 to Equation (53), one can take $\hat{\mathcal{N}}(\alpha)$ as

$$\hat{\mathcal{N}}(\alpha) := 2\Gamma(1-\alpha) \sin(\alpha\pi/2) \pi R_{\text{in}}^2, \quad (56)$$

683 thereby automatically satisfying Equation (55). Then, by using $\hat{\mathcal{N}}(\alpha)$ in Equation (44) in lieu of
684 $\mathcal{N}(\alpha)$, the axial mass flux can be written as

$$\begin{aligned} \hat{y}_\alpha^z(z, t) &= -\frac{\varrho_f}{2\Gamma(1-\alpha) \sin(\alpha\pi/2)} \int_{-\ell(t)}^{+\ell(t)} \frac{1}{|z-\tilde{z}|^\alpha} \mathfrak{d}_\alpha(\tilde{z}, t) \partial_{\tilde{z}} c_a(\tilde{z}, t) d\tilde{z} \\ &= \mathcal{I}_{-\ell(t), +\ell(t)}^{1-\alpha} [-\varrho_f \mathfrak{d}_\alpha \partial_{\tilde{z}} c_a](z, t), \end{aligned} \quad (57)$$

685 where $\mathcal{I}_{-\ell(t), +\ell(t)}^{1-\alpha} [-\varrho_f \mathfrak{d}_\alpha \partial_{\tilde{z}} c_a]$ is the one-dimensional Riesz potential of $-\varrho_f \mathfrak{d}_\alpha \partial_{\tilde{z}} c_a$, but with inte-
686 gration limits $\pm\ell(t)$ instead of $\pm\infty$ (see [104] page 223). For this reason, one may refer to Equation
687 (57) as a “truncated” Riesz potential [38].

688 At this point, two comments are in order. First, we note that, for $\alpha \rightarrow 1^-$, both choices of the
689 normalisation factor lead to the same result and, consequently, the mass flux obtained for $\alpha \rightarrow 1^-$
690 is the same in both formulations. However, something different occurs for $\alpha \rightarrow 0^+$. Indeed, by
691 looking at Equation (46), if the normalisation factor $\mathcal{N}(\alpha)$ is used, we obtain, for $\xi \neq 0$, that

$$\lim_{\alpha \rightarrow 0^+} \mathcal{F}[y_\alpha^z(\cdot, t)](\xi) = 0, \quad (58)$$

692 which suggests that the flux of the species is null for $\alpha \rightarrow 0^+$. On the contrary, if in Equation (46)
693 $\mathcal{N}(\alpha)$ is replaced with $\hat{\mathcal{N}}(\alpha)$, one obtains, for $\xi \neq 0$,

$$\lim_{\alpha \rightarrow 0^+} \mathcal{F}[\hat{y}_\alpha^z(\cdot, t)](\xi) = |\xi|^{-1} \mathcal{F}[-\varrho_f \mathfrak{d}_0(\cdot, t) \partial_z c_a(\cdot, t)](\xi), \quad (59)$$

694 with $\mathfrak{d}_0 = \lim_{\alpha \rightarrow 0^+} \mathfrak{d}_\alpha$, thereby implying, in general, a non-zero flux. In view of the above results and
695 of the normalisation factor used by other Authors[89, 35, 11, 105], we prefer to employ $\mathcal{N}(\alpha)$ as
696 normalisation factor in the remainder of this work. Besides, in this way, the model is able to account
697 for a wider range of diffusion situations, from no diffusion to standard diffusion. Nevertheless, for
698 completeness in our study, in Section “Results and discussion”, we provide a comparison between
699 the approach involving $\mathcal{N}(\alpha)$ and that involving $\hat{\mathcal{N}}(\alpha)$.

700 Now, the restrictions imposed on the motion imply that the only component of interest of the
701 deformation gradient tensor is given by $[\mathbf{F}(X, t)]^z_Z = 1 + u'(Z, t)$. Thus, by taking into account
702 Equation (25), the material fractional diffusivity tensor can be rephrased as follows

$$[\mathfrak{D}_\alpha(X, \tilde{X}, t)]^{ZZ} = \mathfrak{d}_{R\alpha} \frac{1 + u'(\tilde{Z}, t) - J_\gamma(\tilde{Z}, t) \Phi_{s\nu}}{[1 + u'(Z, t)][1 + u'(\tilde{Z}, t)]}, \quad (60)$$

703 whereas the definition (43) implies that \mathfrak{F}_α , given in Equation (22b), can be rephrased as a function
 704 of Z , \tilde{Z} and t , i.e.,

$$\mathfrak{F}_\alpha(X, \tilde{X}, t) = \mathfrak{H}_\alpha(Z, \tilde{Z}, t) = \frac{1}{2\Gamma(1-\alpha)\pi R_{\text{in}}^2} \frac{1}{|Z + u(Z, t) - \tilde{Z} - u(\tilde{Z}, t)|^\alpha}, \quad \alpha \in]0, 1[. \quad (61)$$

705 Finally, by substituting Equation (60) into Equation (23b), and taking into account relation (22b),
 706 the only non-zero component of the material fractional mass flux vector, \mathbf{Y}_α , is the one along the
 707 axial direction, and represents the backward Piola transform of Equation (44), i.e.,

$$Y_\alpha^Z(Z, t) = -\frac{\varrho_f}{2\Gamma(1-\alpha)} \int_{-L_{\text{in}}}^{+L_{\text{in}}} \mathfrak{D}_{R\alpha} \frac{[1 + u'(\tilde{Z}, t) - J_\gamma(\tilde{Z}, t)\Phi_{s\nu}]}{|Z + u(Z, t) - \tilde{Z} - u(\tilde{Z}, t)|^\alpha} \frac{\mathbf{c}'_a(\tilde{Z}, t)}{[1 + u'(\tilde{Z}, t)]} d\tilde{Z}. \quad (62)$$

708 Looking at Equations (61) and (62), we remark that, in contrast to what is usually assumed in the
 709 “standard” setting of Fractional Calculus, both \mathfrak{H}_α and Y_α^Z depend on the displacement field, rather
 710 than depending on the difference between Z and \tilde{Z} , only. As anticipated in the Introduction, this
 711 result is one of the most relevant novelties of our work, as it prescribes that the non-locality evolves
 712 with the change of configuration of the system. Moreover, since in our framework the displacement
 713 is driven by growth (even though u and γ are formally independent variables), we conclude that
 714 the non-locality of the problem is related also to the variation of the tissue’s internal structure, as
 715 modelled by γ .

716 8 Results and discussion

717 In this section, we study the impact of the non-local diffusion of nutrients on the benchmark
 718 problem specified above. For this scope, we distinguish between two mathematical models, both
 719 characterised by Equations (26a)–(26e). The first model, referred to as *fractional model*, describes
 720 the growth of the considered avascular tumour in the case in which the diffusion of the nutrients is
 721 governed by the non-local constitutive law (62). The second model, denominated *standard model*,
 722 describes the growth of the tumour by employing the same governing equations (26a)–(26e), with
 723 the only difference being that the nutrients’ diffusive mass flux vector is expressed by standard
 724 Fick’s law, i.e.,

$$\mathbf{Y}_{\text{std}}(X, t) = -\varrho_f \mathbf{D}(X, t) \text{Grad} \mathbf{c}_a(X, t), \quad (63)$$

725 where “std” stands for “standard”, and \mathbf{D} is the *material diffusivity tensor*, given by [101, 56]

$$\mathbf{D}(X, t) = (J(X, t) - J_\gamma(X, t)\Phi_{s\nu}) d_R \mathbf{C}^{-1}(X, t). \quad (64)$$

726 We notice that both models, i.e., the fractional and the standard one, share the same set of param-
 727 eters except for the reference diffusivities $\mathfrak{D}_{R\alpha}$ and d_R . Note also that Equation (64) can be obtained
 728 from (25) by setting $\tilde{X} = X$ and then taking the limit for $\alpha \rightarrow 1^-$, i.e., $\lim_{\alpha \rightarrow 1^-} \mathfrak{D}_\alpha(X, X, t) =$
 729 $\mathbf{D}(X, t)$.

730 For the purposes of our work, one should not fix $\mathfrak{D}_{R\alpha}$ independently of d_R . Indeed, in order to
 731 compare the results of the non-local model with those of the local one, $\mathfrak{D}_{R\alpha}$ must depend on d_R
 732 in such a way that it tends to d_R in the limit $\alpha \rightarrow 1^-$. For this reason, and taking into account

733 that there exist several experimental works in which the standard diffusivity of species in biological
734 tissues has been measured (see e.g. [62, 59]), we use for $\mathfrak{d}_{R\alpha}$ the definition given in Equation (51),
735 and we set $L = 2L_{\text{in}}$. In Table 1, we provide the list of all the parameters used in our simulations.
736 We remark that, due to the symmetries of the benchmark problem studied in this work, in the
737 following we report the profile of the main quantities of interest restricted to half of the domain,
738 i.e., $[0, L_{\text{in}}]$.

Table 1: List of parameters used in the numerical simulations.

Parameter	Unit	Value	Equation	Reference
L_{in}	cm	0.500	(44)	[101]
R_{in}	cm	$1.000 \cdot 10^{-2}$	(62)	[101]
λ	Pa	$1.333 \cdot 10^4$	(12)	[111]
μ	Pa	$1.999 \cdot 10^4$	(12)	[111]
k_{R}	$\text{m}^2/(\text{Pa}\cdot\text{s})$	$4.875 \cdot 10^{-13}$	(15)	[62]
m_0	—	0.0848	(15)	[62]
m_1	—	4.638	(15)	[62]
d_{R}	m^2/s	$3.200 \cdot 10^{-9}$	(51)	[107]
ζ_{fp}	$\text{kg}/(\text{m}^3\text{s})$	$1.343 \cdot 10^{-3}$	(27a)	[25]
ζ_{nf}	$\text{kg}/(\text{m}^3\text{s})$	$1.150 \cdot 10^{-5}$	(27b)	[25]
ζ_{cp}	$\text{kg}/(\text{m}^3\text{s})$	$3.000 \cdot 10^{-4}$	(27c)	[23, 24]
ζ_{pn}	$\text{kg}/(\text{m}^3\text{s})$	$1.500 \cdot 10^{-3}$	(27d)	[25]
\mathfrak{c}_{cr}	—	$1.000 \cdot 10^{-3}$	(27a)	[101]
$\mathfrak{c}_{\text{env}}$	—	$7.000 \cdot 10^{-3}$	(27a)	[101]
\mathfrak{c}_0	—	$1.000 \cdot 10^{-2}$	(27c)	This work
δ_1	—	$7.138 \cdot 10^{-1}$	(27a)	[80]
δ_2	Pa	$1.541 \cdot 10^3$	(27a)	[80]
$\Phi_{s\nu}$	—	0.8	(5a)	[101]
ϱ_{s}	kg/m^3	1000	(2)	[101]
ϱ_{f}	kg/m^3	1000	(2)	[101]

739 To start with, in Fig. 1, we report the spatial profile of the nutrients' mass fraction $\mathfrak{c}_a(Z, t)$.
740 Specifically, in the left panel of Fig. 1, we present the results of our simulations for $\alpha = 0.1$ (dashed
741 line) and $\alpha = 0.9$ (solid line), and for different times. As shown in this plot, the parameter α permits
742 to control how the nutrients diffuse into the tumour from the axial boundaries (i.e., the terminal
743 cross sections $Z = \pm L_{\text{in}}$). In particular, for $\alpha = 0.1$ the diffusion of the nutrients is constrained to
744 the tumour's axial boundary, i.e., close to $Z = \pm L_{\text{in}}$, so that their mass fraction is dramatically
745 reduced in the internal points of the specimen. In such a situation, the proliferating cells consume
746 the nutrients that are already present in the tissue, without the replenishment needed to continue
747 their proliferation. On the contrary, for $\alpha = 0.9$, the nutrients are able to diffuse towards the centre
748 of the tumour, so that their consumption is less localised. For clarity, in the plot we prefer to show
749 only the curves corresponding to $\alpha = 0.1$ and $\alpha = 0.9$. For any other value of $\alpha \in]0.1, 0.9[$, the
750 model is able to describe different diffusion profiles ranging between the ones obtained for $\alpha = 0.1$
751 and for $\alpha = 0.9$. To us, an interesting feature of the curves corresponding to $\alpha = 0.1$ is that,
752 depending on the point Z at which the nutrients' mass fraction is observed, the trend of these

753 curves exhibits a different monotonicity in time. Indeed, the nutrients' mass fraction decreases in
754 time close to the boundary $Z = L_{\text{in}}$, whereas it increases towards the tumour's centre. Furthermore,
755 in the panel on the right of Fig. 1, we compare, for different values of α , the results obtained with
756 the fractional model with those obtained with the standard model at time $t = 20$ d. Specifically, for
757 α close to 0, there is almost no diffusion, while, when α is close to 1, the fractional model conducts
758 to the standard one, as evidenced by our previous calculations (see Equation (46)).

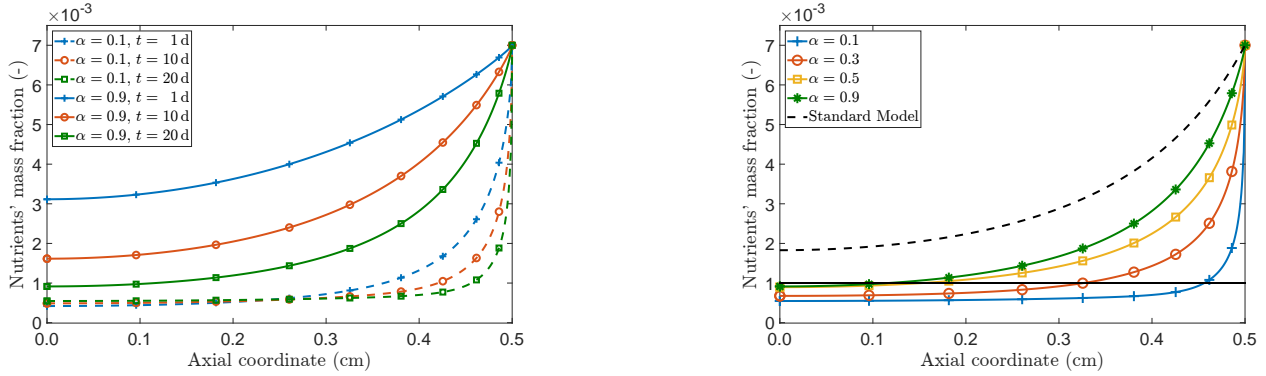


Figure 1: Spatial profile of the nutrients' mass fraction $c_a(Z, t)$ for different values of α and at different times (panel on the left), and comparison of the results obtained with the fractional and the standard model at time $t = 20$ d (panel on the right).

759 As shown in Fig. 2, the non-local way in which the nutrients diffuse into the tissue affects
760 the manner in which the tumour grows. By increasing α and, thus, enhancing diffusion, one also
761 increases the availability of the nutrients in the tumour, thereby boosting its growth. On the
762 other hand, for $\alpha = 0.1$, the displacement is hindered and its highest values are attained in a
763 neighbourhood of $Z = L_{\text{in}}$. Indeed, this is where the nutrients enter the tumour and their mass
764 fraction still remains high enough to trigger growth, so that the magnitude of the displacement in
765 this region of the tumour is higher than elsewhere. However, moving towards the interior of the
766 tumour, the fact that the nutrients' concentration is below the critical threshold brings growth to
767 a stop, thereby considerably reducing the magnitude of the displacement. This behaviour shows
768 that also the monotonicity in time of the displacement curves depends on the point Z at which
769 they are reckoned. More in detail, the reduction of the displacement in the interior of the tumour
770 may be due to the loss of mass caused by the lack of nutrients, which implies that the proliferating
771 cells start to die, and a region of necrotic cells comes into sight. This behaviour becomes even more
772 evident by looking at the left panel of Fig. 3. Moreover, comparing the right panels of Fig. 1 and
773 Fig. 3, we notice that the part of the domain in which the necrotic cells appear coincides with the
774 one in which the nutrients fall below the critical value c_{cr} , represented with the solid horizontal line
775 in the right panel of Fig. 1. By referring to Equation (27d), when $c_a < c_{\text{cr}}$, the rate of mass R_{pn}
776 becomes active and, therefore, the proliferating cells change into necrotic cells.

777 To continue our analysis, we refer to Fig. 4, where we plot the growth parameter γ . By focusing
778 on the panel on the left, we notice, for $\alpha = 0.1$, a localisation of the variation of the growth
779 parameter near the boundary $Z = L_{\text{in}}$ for increasing time, whereas, for $\alpha = 0.9$, the variation of
780 γ is more uniformly distributed in the whole domain. Besides, for $\alpha = 0.1$, γ is greater than one
781 for all $Z \in [0, L_{\text{in}}]$ and for all t , even though this is difficult to be observed with the unaided eye.

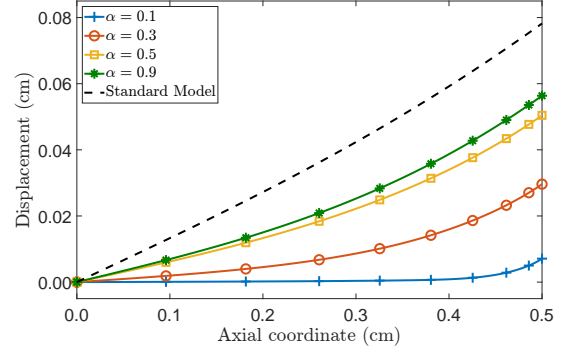
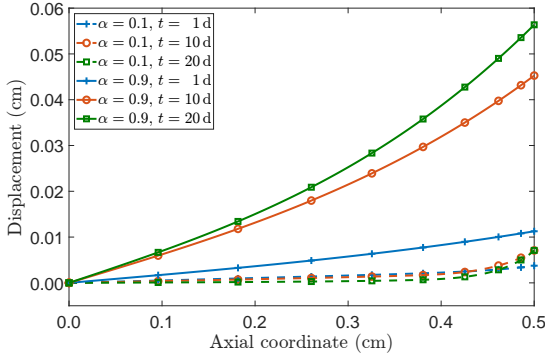


Figure 2: Spatial profile of the axial displacement $u(Z,t)$ for different values of α and at different times (panel on the left), and comparison of the results obtained with the fractional and the standard model at time $t = 20$ d (panel on the right).

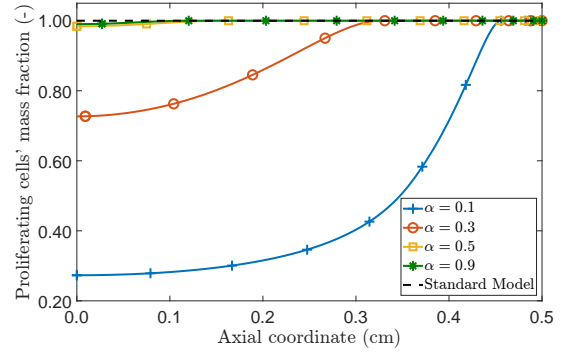
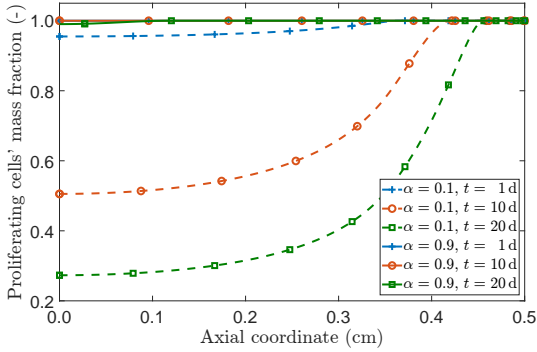


Figure 3: Spatial profile of the proliferating cells' mass fraction $c_p(Z,t)$ for different values of α and at different times (panel on the left), and comparison of the results obtained with the fractional and the standard model at time $t = 20$ d (panel on the right).

782 This is because, although for $t \geq 1$ d the mass fraction of the nutrients is above the threshold
783 value c_{cr} mostly near the boundary (see the left panel of Fig. 1), the inner region has undergone
784 a growth process at earlier times. Indeed, since the condition $c_a(Z,0) \equiv c_{env} > c_{cr}$ is respected,
785 the mass rate R_{fp} is greater than zero, and we can conclude that, from the very beginning, the cell
786 proliferation is promoted until the nutrients' concentration falls below its critical value. Note also
787 that this is accelerated when α is near zero because of the slow pace with which the nutrients are
788 refilled. At this point, the proliferating cells abruptly die, thereby turning into necrotic cells, and
789 go into the fluid (see the definition of R_{nf}), which results in a loss of mass. For $\alpha = 0.9$, instead, it
790 is visible also with the naked eye that γ is greater than unity everywhere in $[0, L_{in}]$ and for all the
791 considered times. Finally, as noticed for the nutrients' mass fraction and for the displacement, also
792 the monotonicity in time of the trend of the growth parameter depends, for $\alpha = 0.1$, on the point
793 Z at which γ is observed. Indeed, γ is monotonically increasing in time for Z close to $Z = L_{in}$, and
794 monotonically decreasing for Z "moving" towards the centre of the tumour.

795 Now, we report the evolution of the pressure, p , in Fig. 5. For both the standard and the
796 fractional model, when α is close to 1, the pressure of the interstitial fluid decreases, taking negative

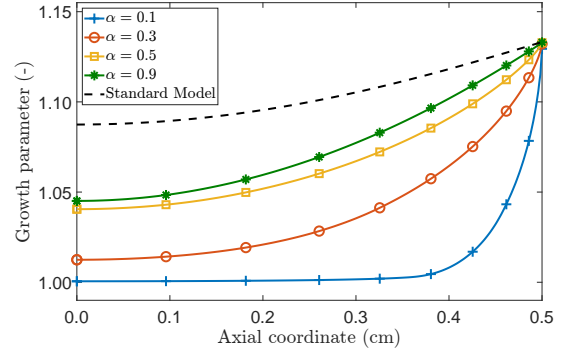
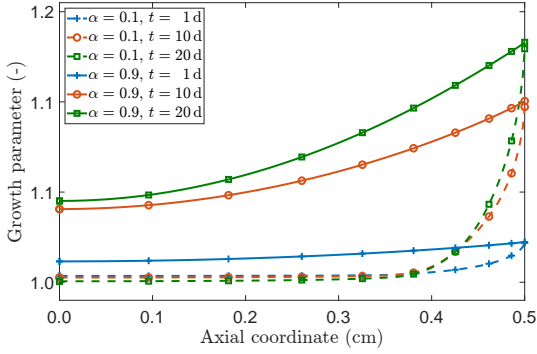


Figure 4: Spatial profile of the growth parameter $\gamma(Z, t)$ for different values of α and at different times (panel on the left), and comparison of the results obtained with the fractional and the standard model at time $t = 20$ d (panel on the right).

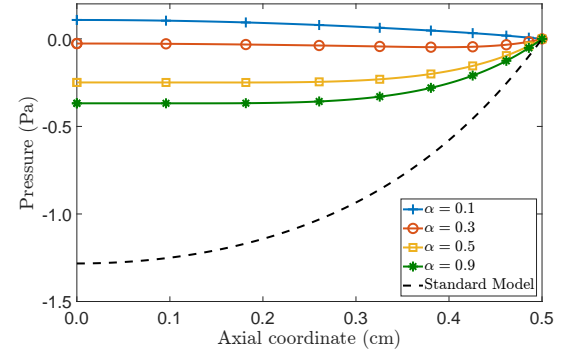
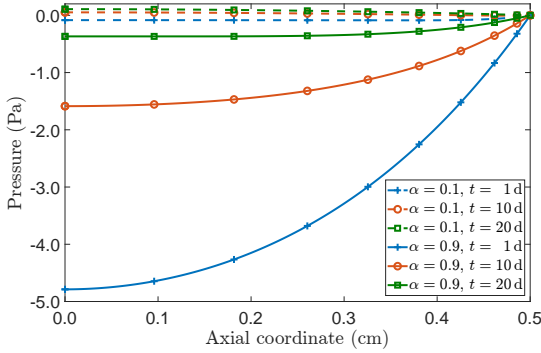


Figure 5: Spatial profile of the pressure $\mathbf{p}(Z, t)$ for different values of α and at different times (panel on the left), and comparison of the results obtained by the fractional and the standard model at time $t = 20$ d (panel on the right).

797 values, from the free boundary towards the tumour's centre. However, for α tending towards 0 from
798 above, the pressure in the interior of the tumour tends to become positive. To explain this event,
799 we notice that the proliferating cells absorb fluid from the surrounding environment to fuel their
800 growth, which is possible because the fluid flows towards the tumour's interior. However, due to
801 an over-consumption of nutrients, the level of those drastically decreases in the innermost zone
802 of the tumour. This situation, as evidenced in our simulations (see Fig. 4), creates a layer of
803 proliferating cells near the outer surface (i.e., the cross section $Z = L_{\text{in}}$), and a region of necrotic
804 cells at the centre of the tumour. By looking at Equation (27b), in this circumstance, the necrotic
805 cells dissolve into the fluid with rate ζ_{nf} , thereby increasing its pressure, which, in turn, generates
806 an outward flux (i.e., a flux in the direction opposite to the fluid flow). This sequence of events,
807 which are consistent with the biological foundations of nutrient diffusion and necrosis in a tumour
808 as explained in [77], arises in the model thanks to the non-local approach presented in this work.
809 That is, the non-locality parameter α is responsible for this picture and, thus, through its inclusion,
810 the fractional model is able to reproduce a scenario that was not initially considered in the model.
811 On the contrary, as the results show, this behaviour would not be observed within a formulation

812 based on standard Fick's law, at least with our model as is.

813 Finally, as we mentioned before (see Remark 3), for completeness in our discussion, we compare
814 the results corresponding to the adoption of $\mathcal{N}(\alpha)$ versus those obtained with $\hat{\mathcal{N}}(\alpha)$. As shown
815 in Fig. 6, top left panel, when the normalisation factor is $\hat{\mathcal{N}}(\alpha)$, we observe, for $\alpha \rightarrow 0^+$, a less
816 pronounced decrease of the nutrients' mass fraction. This is compatible with the fact that, even for
817 very small values of α , there is an incoming mass flux of nutrients through the domain's boundaries
818 that reestablishes the nutrients eaten by the cells. This effect, in turn, tends to disappear when
819 the normalisation factor $\mathcal{N}(\alpha)$ is employed since, in that case, the mass flux tends to zero in the
820 limit $\alpha \rightarrow 0^+$. Coherently with this observation, we also notice a markedly different behaviour of
821 the growth parameter (see Fig. 6, top right panel). Indeed, since the flux of nutrients obtained
822 for $\hat{\mathcal{N}}(\alpha)$ does not vanish for $\alpha \rightarrow 0^+$, and a greater amount of nutrients remains available even
823 at time $t = 20$ d, growth can still occur, as is testified by the dotted line marked with "+".
824 Similar comments pertain also to the description of the displacement (see Fig. 6, bottom left
825 panel). Indeed, since growth remains active also for small values of α , the displacement also tends
826 to persist even at $t = 20$ d, and remains relatively large in the neighbourhood of the domain's
827 boundaries, where the availability of nutrients is the highest (because of the Dirichlet condition
828 assigned to the nutrients' mass fraction) and growth is present. These differences notwithstanding,
829 it should be emphasised that the qualitative behaviour of the curves describing the nutrients' mass
830 fraction and the growth parameter is the same for both choices of the normalisation factor. On the
831 contrary, the behaviour of the pressure (see Fig. 6, bottom right panel) is *both* qualitatively *and*
832 quantitatively different for $\alpha = 0.1$. In fact, the use of $\hat{\mathcal{N}}(\alpha)$ nullifies the effect visible at $t = 20$ d,
833 for $\alpha = 0.1$ and normalisation factor $\mathcal{N}(\alpha)$, which consisted in the sign change of the pressure.
834 Hence, employing $\hat{\mathcal{N}}(\alpha)$ leaves the pressure negative, thereby triggering no inversion in the flow of
835 the interstitial fluid, which continues to flow from the exterior of the tumour into it.

836 9 Conclusions

837 In this work, we study the influence of a given type of non-local diffusion of nutrients on the growth
838 of an avascular tumour. For this purpose, we generalise Fick's law of diffusion by introducing a
839 non-local constitutive relationship for the mass flux vector that, after some considerations, can be
840 identified with a fractional derivative of the nutrients' mass fraction. We call attention to the fact
841 that, since we are dealing with growth, we need to describe how the non-locality of the prescribed
842 constitutive law evolves with the deformation and the growth-induced inelastic distortions that
843 accompany the evolution of the system under study. This consideration implies that the non-
844 locality of the presumed constitutive response should be subordinate to the motion χ (see Equation
845 (22b)) and, thus, that it cannot depend explicitly on the difference $X - \tilde{X}$ between the reference
846 placements of the material points embedded in X and \tilde{X} . Furthermore, we note that, as prescribed
847 by Equation (25), the non-local character of the mass flux vector also depends on the structural
848 changes of the tumour through the determinant of \mathbf{F}_γ . To the best of our understanding, the above
849 considerations imply substantial differences between our work and other papers on the subject
850 found in the scientific literature. Moreover, we suggest a formulation of non-local diffusion on
851 manifolds (see Appendix A1).

852 To investigate the influence of the non-local diffusion of the nutrients on the tumour evolution,
853 we focused on a benchmark problem that allows, due to the enforced symmetries, the reduction

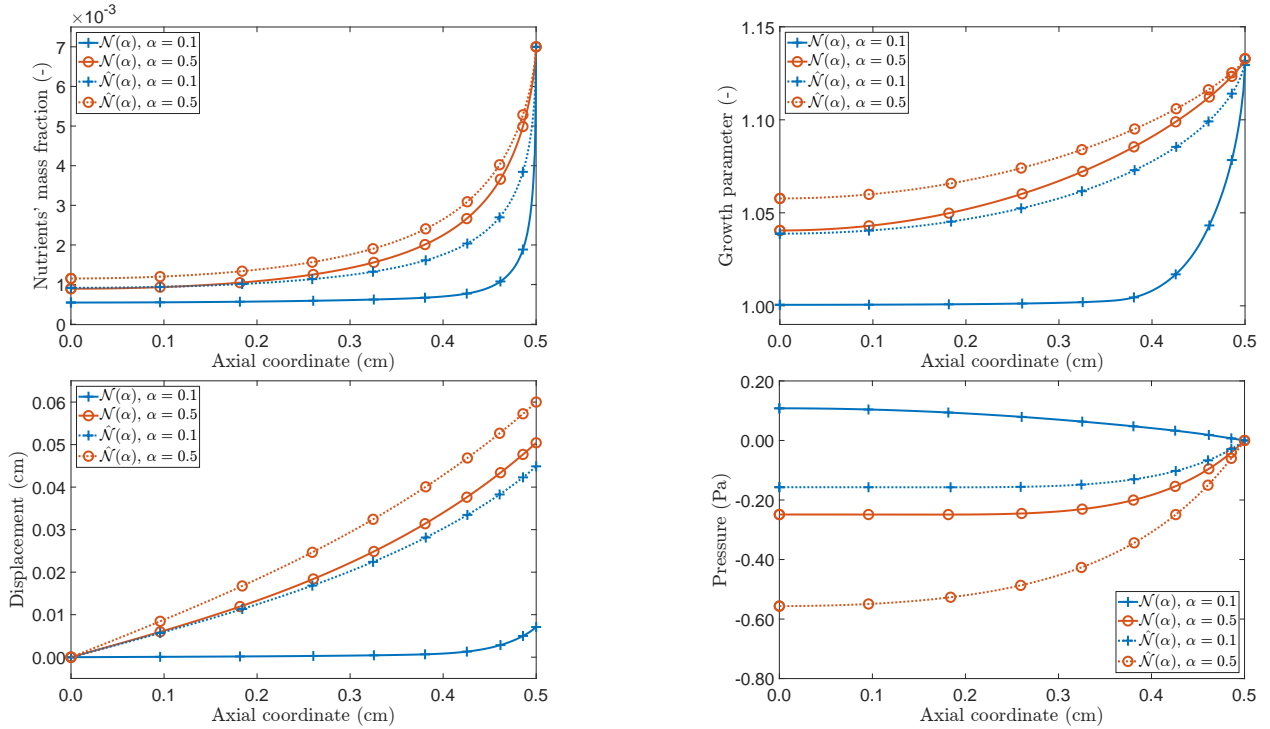


Figure 6: Comparison of the spatial profiles of $\mathbf{c}_a(Z, t)$ (top left), $\gamma(Z, t)$ (top right), $u(Z, t)$ (bottom left) and $\mathbf{p}(Z, t)$ (bottom right) for the approaches involving $\mathcal{N}(\alpha)$ (solid line) and $\hat{\mathcal{N}}(\alpha)$ (dotted line). In the plots different values of α are used and time is fixed to $t = 20$ d.

854 of the original three-dimensional framework to a one-dimensional problem. This has an important
 855 impact on the selection of the non-locality function, \hat{f}_α , which has to be able to capture how the
 856 geometrical symmetries of the problem affect the description of the non-locality. Particularly, in
 857 our analysis, we re-obtained the definition of one-dimensional fractional mass flux proposed in other
 858 works [89, 35].

859 In our work, the numerical solution of the set of equations defining the mathematical model
 860 is found by employing the FE method, which has been adapted for the solution of the fractional
 861 diffusion equation (26c). In particular, the obtained numerical results show that the non-local
 862 character of the nutrients' evolution has a considerable repercussion on the growth of the hypo-
 863 theoretical tumour under study. Specifically, by varying the parameter $\alpha \in]0, 1[$, the model is capable,
 864 in the limit cases, of generating situations of no diffusion or of restoring Fick's law. This conclu-
 865 sion evidences the relevance of embracing a fractional framework in our model, since it permits to
 866 "control", through the parameter α , the way in which the tumour grows. Finally, we discussed a
 867 possible way for defining another normalisation factor, termed $\hat{\mathcal{N}}(\alpha)$, involved in the definition of
 868 the mass flux vector, and we provided a comparison between the two approaches.

869 Certainly, our model can be further generalised and, in the following, we discuss some important
 870 issues that should be accounted for in forthcoming works. A first issue arises from the fact that,
 871 once the dimensionality and the symmetries of the problem at hand are specified, Equation (16)
 872 must be adapted accordingly. This implies that the non-locality function and the normalisation

873 factors should be conceived in a symmetry- and dimensional-dependent fashion². To find such
874 relations is part of our ongoing research. Additionally, in our model, the information on the
875 microscopic structure of the tumour is not explicitly taken into account and, thus, its contribution
876 is neglected. As pointed out in the Introduction, the multi-scale and heterogeneous character of the
877 environment in which diffusion takes place is one of the main factors influencing the occurrence of
878 non-Fickian diffusion. Therefore, the adoption of mathematical techniques, such as the Asymptotic
879 Homogenisation Method [29], could be capable of incorporating these features into a framework of
880 tissue growth [96] and non-local diffusion.

881 We further remark that an aspect that is not contemplated in the current formulation of the
882 model is that the chemical agents should be both in the fluid phase and in the solid phase, and not
883 only in the fluid phase. One of the main drawbacks of this phenomenological consideration is that it
884 is not possible to link the mass sources to the chemical potentials of the nutrients, nor is it possible
885 to establish a sound and comprehensive thermodynamic framework accounting for interphase mass
886 transfers as non-equilibrium processes. This implies that no information, or only a limited amount
887 of information, can be extracted from the study of the dissipation inequality of the system (and this
888 is not directly due to the fact that growth necessitates the consideration of processes, of cellular or
889 molecular type, that could not be accounted for in the model). Therefore, under the circumstances
890 of the present model, it is not possible to obtain Equation (16) from the study of the dissipation
891 inequality, as it would be the case in the classical procedure that leads to Fick’s law. In this respect,
892 one of the technical difficulties that arise in our work is that we cannot invert the balance of linear
893 momentum associated with the chemical agents, since the inversion of fractional operators is not
894 always permitted. One possible solution, that seems to be thermodynamically acceptable, is to
895 adopt a procedure similar to the one depicted in [58], that is, to consider the part of the dissipation
896 inequality that is of interest for us, to put it in weak form and to express the flux in terms of a
897 non-local constitutive law depending on the gradient of the chemical potential.

898 Finally, we would like to mention that in recent years Fractional Calculus has demonstrated to
899 be an effective mathematical tool in the description of several phenomena. However, there is still
900 an urgency in incorporating this notion in mathematical models that go beyond the classical ones.

901 **Acknowledgement**

902 The Authors acknowledge the *Dipartimento di Scienze Matematiche* (DISMA) “G.L. Lagrange” of
903 the *Politecnico di Torino*, and that the present research has been partially supported by MIUR
904 grant “Dipartimenti di Eccellenza 2018–2022” (‘Departments of Excellence 2018–2022’), project
905 no. E11G18000350001. The Authors warmly thank Prof. Dušan Zorica for his invaluable help, for
906 providing essential references and for the many suggestions that he has given us for this work.

907 **Authors contribution**

908 All Authors have equally contributed to this work.

²Similar problems are subject of investigations conducted by our group in conjunction with our colleague Prof. Dušan Zorica (Mathematical Institute, Serbian Academy of Arts and Sciences, Serbia) and started, from our side, during his visit at the *Politecnico di Torino* (Italy) in January 2020.

909 Conflict of Interests

910 The Authors declare that they have no conflict of interests.

911 A A1 Some aspects of non-locality on manifolds

912 In the following, we propose a possible way for the formulation of non-local diffusion on manifolds.
 913 For this purpose, let us recall that the fractional mass flux vector \mathbf{y}_α is defined through the duality
 914 product

$$\langle \mathbf{y}_\alpha, \text{grad } \check{c} \rangle := -\varrho_f \int_{\mathcal{B}_t} \left\{ \int_{\mathcal{B}_t} [\text{grad } \check{c}(x)] \mathbf{d}_\alpha(x, \tilde{x}, t) [\text{grad } c_a(\tilde{x}, t)] dv(\tilde{x}) \right\} dv(x), \quad (65a)$$

$$\mathbf{d}_\alpha(x, \tilde{x}, t) := \mathfrak{f}_\alpha(x, \tilde{x}) \mathfrak{d}_\alpha(x, \tilde{x}, t), \quad (65b)$$

915 where the non-locality function is given by the following relationship

$$\mathfrak{f}_\alpha(x, \tilde{x}) := \mathfrak{f}_\alpha^{(0)}(x_0, \mathcal{T}_x^{x_0}(\tilde{x})). \quad (66)$$

916 In Equation (66), the notation $\mathcal{T}_x^{x_0} := \exp_{x_0} \circ (\mathcal{P}_{x_0}^x)^{-1} \circ \exp_x^{-1}$ is used, and the following operators
 917 are introduced:

- 918 • Let $T_{x,\delta}\mathcal{B}_t$ be the subset of the tangent space $T_x\mathcal{B}_t$ defined by

$$T_{x,\delta}\mathcal{B}_t := \{\mathbf{v}_x \in T_x\mathcal{B}_t \mid \langle \mathbf{v}_x, \mathbf{v}_x \rangle_{\mathbf{g}} \leq \delta, \text{ with } \delta > 0\}, \quad (67)$$

919 and let $\mathcal{U}_t(x, \delta) := \{\tilde{x} \in \mathcal{B}_t \mid \text{dist}_{\mathcal{B}_t}(x, \tilde{x}) \leq \delta\}$ be a closed neighbourhood of x having radius
 920 δ , with $\text{dist}_{\mathcal{B}_t} : \mathcal{B}_t \times \mathcal{B}_t \rightarrow \mathbb{R}_0^+$ denoting the *distance function*³ on \mathcal{B}_t [106]. The operator

$$\exp_x : T_{x,\delta}\mathcal{B}_t \rightarrow \mathcal{U}_t(x, \delta), \quad (68)$$

921 referred to as *exponential map*, is injective and associates each element of $T_{x,\delta}\mathcal{B}_t$ with the
 922 point $\tilde{x} = \exp_x(\mathbf{v}_x) \in \mathcal{U}_t(x, \delta)$, which is the projection of \mathbf{v}_x onto $\mathcal{U}_t(x, \delta)$. Note that the
 923 result of this operation generalises the concept of translation to the case of a manifold. To
 924 construct $\exp_x(\mathbf{v}_x)$, we take $\mathbf{v}_x \in T_{x,\delta}\mathcal{B}_t$ and consider the unique solution to the geodesic
 925 equation (see e.g. [79]), parameterised by $\eta : [0, 1] \rightarrow \mathcal{U}_t(x, \delta)$, and in harmony with the
 926 “initial” conditions $\eta(0) = x$ and $\eta'(0) = \mathbf{v}_x$. Then, we identify $\exp_x(\mathbf{v}_x)$ with $\eta(1)$, i.e.,
 927 $\exp_x(\mathbf{v}_x) = \eta(1) \equiv \tilde{x}$.

928 By construction, the exponential map is invertible and its inverse, i.e., $\exp_x^{-1} : \mathcal{U}_t(x, \delta) \rightarrow$
 929 $T_{x,\delta}\mathcal{B}_t$, returns a unique tangent vector of $T_{x,\delta}\mathcal{B}_t$ for each point of $\mathcal{U}_t(x, \delta)$. Therefore, by
 930 taking $\tilde{x} \in \mathcal{U}_t(x, \delta)$, with $\tilde{x} = \eta(1)$, it holds that $\exp_x^{-1}(\eta(1)) = \eta'(0)$.

931

³Given the geodesic from x to \tilde{x} , and denoting by $\eta : [0, 1] \rightarrow \mathcal{B}_t$ its parameterisation, so that $x = \eta(0)$
 and $\tilde{x} = \eta(1)$, we set $\text{dist}_{\mathcal{B}_t}(x, \tilde{x}) := \int_0^1 \|\eta'(\sigma)\| d\sigma$.

932 • Let us consider two points of the manifold, e.g. $x_0, x \in \mathcal{B}_t$, and let $\zeta : [0, s] \rightarrow \mathcal{B}_t$, with
 933 $\zeta(0) = x_0$ and $\zeta(s) = x$, be the parameterisation of the geodesic connecting x_0 to x . Moreover,
 934 let us take the sets of tangent vectors $T_{x_0, \delta} \mathcal{B}_t$ and $T_{x, \delta} \mathcal{B}_t$, with $\delta > 0$. Then, to transport
 935 parallelly the elements of $T_{x_0, \delta} \mathcal{B}_t$ into $T_{x, \delta} \mathcal{B}_t$ along the geodesic parameterised by ζ , we define
 936 the shifter operator

$$\mathcal{P}_{x_0}^x : T_{x_0, \delta} \mathcal{B}_t \rightarrow T_{x, \delta} \mathcal{B}_t, \quad \mathbf{v}_{x_0} \mapsto \mathcal{P}_{x_0}^x \mathbf{v}_{x_0} = \mathbf{v}_x. \quad (69)$$

937 Clearly, $\mathcal{P}_{x_0}^x$ is invertible and its inverse reads $(\mathcal{P}_{x_0}^x)^{-1} = \mathcal{P}_{x_0}^{x_0} : T_{x, \delta} \mathcal{B}_t \rightarrow T_{x_0, \delta} \mathcal{B}_t$. In addition,
 938 $\mathcal{P}_{x_0}^{x_0}$ is the identity operator from $T_{x_0, \delta} \mathcal{B}_t$ into itself.

939

940 • To represent $\mathfrak{f}_\alpha(x, \tilde{x})$ properly, we explain in detail our understanding of the procedure
 941 sketched in [106]. For this purpose, we start recalling that $\mathfrak{f}_\alpha(x, \tilde{x})$ measures how, at time t ,
 942 the value of $\text{grad} c_a(\tilde{x}, t)$ is “felt” at x , for all pairs of points $x, \tilde{x} \in \mathcal{B}_t$, such that $\tilde{x} \in \mathcal{U}_t(x, \delta)$,
 943 with $\delta > 0$. This influence has to be described in a way respectful of the geometry of the
 944 manifold, which can be achieved as follows. Given $\mathfrak{f}_\alpha(x, \tilde{x})$, we select arbitrarily a point
 945 $x_0 \in \mathcal{B}_t$ and we introduce an auxiliary function $\mathfrak{f}_\alpha^{(0)}(x_0, \cdot) : \mathcal{U}_t(x_0, \delta) \rightarrow \mathbb{R}$, such that, for an
 946 appropriate $\tilde{x}_0 \in \mathcal{U}_t(x_0, \delta)$, $\mathfrak{f}_\alpha^{(0)}(x_0, \tilde{x}_0) = \mathfrak{f}_\alpha(x, \tilde{x})$. In order for \tilde{x}_0 to be “appropriate”, it has
 947 to depend on x and \tilde{x} (and on x_0). This can be obtained by calling for the operator

$$\mathcal{T}_x^{x_0} := \exp_{x_0} \circ (\mathcal{P}_{x_0}^x)^{-1} \circ \exp_x^{-1} : \mathcal{U}_t(x, \delta) \rightarrow \mathcal{U}_t(x_0, \delta). \quad (70)$$

948 As anticipated above, for each $\tilde{x} \in \mathcal{U}_t(x, \delta)$, \exp_x^{-1} returns a vector \mathbf{v}_x , such that $\|\mathbf{v}_x\| \leq \delta$.
 949 Then, $(\mathcal{P}_{x_0}^x)^{-1}$ transports \mathbf{v}_x parallelly to x_0 , so that $(\mathcal{P}_{x_0}^x)^{-1} \mathbf{v}_x = \mathbf{v}_{x_0}$. Finally, the operator
 950 \exp_{x_0} maps \mathbf{v}_{x_0} into $\tilde{x}_0 = \exp_{x_0}(\mathbf{v}_{x_0}) \in \mathcal{U}_t(x_0, \delta)$. Therefore, it holds that $\tilde{x}_0 = \mathcal{T}_x^{x_0}(\tilde{x})$,
 951 thereby explaining how \tilde{x}_0 depends on x and \tilde{x} , for a given x_0 . More specifically, the action
 952 of $\mathcal{T}_x^{x_0}$ on \tilde{x} permits to find the only \tilde{x}_0 such that Equation (66) becomes

$$\mathfrak{f}_\alpha(x, \tilde{x}) = \mathfrak{f}_\alpha^{(0)}(x_0, \mathcal{T}_x^{x_0}(\tilde{x})) = \mathfrak{f}_\alpha^{(0)}(x_0, \tilde{x}_0), \quad (71)$$

953 where the composition $\mathfrak{f}_\alpha(x, \cdot) = \mathfrak{f}_\alpha^{(0)}(x_0, \cdot) \circ \mathcal{T}_x^{x_0} : \mathcal{U}_t(x, \delta) \rightarrow \mathbb{R}$ is implied. The essence of
 954 this result is that the information on the non-locality of a given phenomenon between x and
 955 \tilde{x} , encompassed by $\mathfrak{f}_\alpha(x, \tilde{x})$, is “transported” to the pair of points x_0 and \tilde{x}_0 (see Fig. 7).

956 To conclude, we notice that, in an affine space or, more generally, in a flat subset of an affine
 957 space, the procedure outlined above boils down to the determination of the unique point \tilde{x}_0
 958 such that $\mathbf{v}_{x_0} = \tilde{x}_0 - x_0$ is equipollent to $\mathbf{v}_x = \tilde{x} - x$, for given x_0, x and \tilde{x} . Indeed, within
 959 this framework, $\mathcal{T}_x^{x_0}$ operates in such a way that $\mathbf{v}_{x_0} = \mathcal{T}_x^{x_0}(\tilde{x}) - x_0 = \tilde{x}_0 - x_0$ is parallel to \mathbf{v}_x
 960 (because \mathbf{v}_x is transported parallelly along the geodesic —now, a straight line— connecting x
 961 with x_0) and $\|\mathbf{v}_{x_0}\| \equiv \|\tilde{x}_0 - x_0\| = \|\tilde{x} - x\| \equiv \|\mathbf{v}_x\|$. Moreover, $\mathfrak{f}_\alpha(x, \tilde{x})$ and $\mathfrak{f}_\alpha^{(0)}(x_0, \tilde{x}_0)$ can be
 962 rephrased as $\mathfrak{f}_\alpha(x, \tilde{x}) = \hat{\mathfrak{f}}_\alpha(x - \tilde{x})$ and $\mathfrak{f}_\alpha^{(0)}(x_0, \tilde{x}_0) = \hat{\mathfrak{f}}_\alpha(x_0 - \tilde{x}_0)$, respectively, and Equation
 963 (66), or Equation (71), is trivially satisfied. In this respect, we say that Equation (66) adapts
 964 the meaning of convolution from the case of an affine space to the case of a manifold (see
 965 Fig. 8).

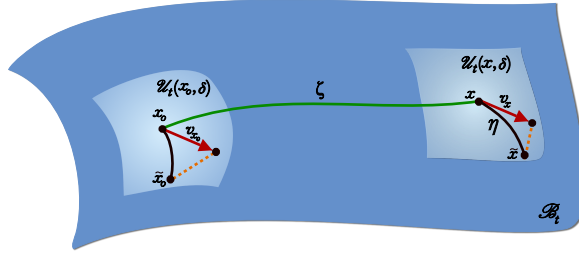


Figure 7: The convolution on manifolds is defined by transporting $f_\alpha(x, \cdot) : \mathcal{U}_t(x, \delta) \rightarrow \mathbb{R}$ to every point of \mathcal{B}_t , while taking into account the manifold geometry. Thus, given a point $\tilde{x} = \eta(1) \in \mathcal{U}_t(x, \delta)$, the operation $\exp_x^{-1}(\tilde{x})$ returns the vector $\mathbf{v}_x = \eta'(0)$, which is parallelly transported to \mathbf{v}_{x_0} through a geodesic $\zeta : [0, s] \rightarrow \mathcal{B}_t$ connecting $x = \zeta(s)$ and $x_0 = \zeta(0)$, and the operation $\exp_{x_0}(\mathbf{v}_{x_0})$ returns the point $\tilde{x}_0 \in \mathcal{U}_t(x_0, \delta)$. In this way, $f_\alpha(x, \cdot)$ is transported from $\mathcal{U}_t(x, \delta)$ to $\mathcal{U}_t(x_0, \delta)$.

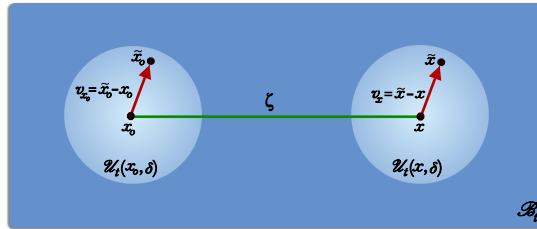


Figure 8: In a flat subset of an affine space $\mathbf{v}_{x_0} = \tilde{x}_0 - x_0$ is equipollent to $\mathbf{v}_x = \tilde{x} - x$. Therefore, $f_\alpha(x, \tilde{x})$ and $f_\alpha^{(0)}(x_0, \tilde{x}_0)$ can be rephrased as $f_\alpha(x, \tilde{x}) = \hat{f}_\alpha(x - \tilde{x})$ and $f_\alpha^{(0)}(x_0, \tilde{x}_0) = \hat{f}_\alpha^{(0)}(x_0 - \tilde{x}_0)$.

966 References

- 967 [1] Fayçal Ben Adda. La différentiabilité dans le calcul fractionnaire. *Comptes Rendus de*
968 *l'Académie des Sciences - Series I - Mathematics*, 326(7):787–791, apr 1998.
- 969 [2] Elias C Aifantis and James B Serrin. The mechanical theory of fluid interfaces and maxwell's
970 rule. *Journal of Colloid and Interface Science*, 96(2):517–529, dec 1983.
- 971 [3] Gioacchino Alotta, Mario Di Paola, Francesco Paolo Pinnola, and Massimiliano Zingales. A
972 fractional nonlocal approach to nonlinear blood flow in small-lumen arterial vessels. *Mecca-*
973 *nica*, 55(4):891–906, mar 2020.
- 974 [4] D. Ambrosi, G.A. Ateshian, E.M. Arruda, S.C. Cowin, J. Dumais, A. Goriely, G.A. Holzapfel,
975 J.D. Humphrey, R. Kemkemer, E. Kuhl, J.E. Olberding, L.A. Taber, and K. Garikipati.
976 Perspectives on biological growth and remodeling. *Journal of the Mechanics and Physics of*
977 *Solids*, 59(4):863–883, apr 2011.
- 978 [5] D. Ambrosi and F. Mollica. On the mechanics of a growing tumor. *International Journal of*
979 *Engineering Science*, 40(12):1297–1316, jul 2002.

- 980 [6] D. Ambrosi and L. Preziosi. On the closure of mass balance models for tumor growth.
981 *Mathematical Models and Methods in Applied Sciences*, 12(05):737–754, may 2002.
- 982 [7] D. Ambrosi, L. Preziosi, and G. Vitale. The insight of mixtures theory for growth and
983 remodeling. *Z. Angew. Math. Phys.*, 61:177–191, 2010.
- 984 [8] R. P. Araujo and D. L. McElwain. A history of the study of solid tumour growth: the
985 contribution of mathematical modelling. *Bulletin of Mathematical Biology*, may 2004.
- 986 [9] T. M. Atanacković, S. Pilipović, B. Stanković, and D. Zorica. *Fractional Calculus with*
987 *Applications in Mechanics: Vibrations and Diffusion Processes*. ISTE Ltd., 2014.
- 988 [10] T M Atanackovic, S Pilipovic, and D Zorica. A diffusion wave equation with two frac-
989 tional derivatives of different order. *Journal of Physics A: Mathematical and Theoretical*,
990 40(20):5319–5333, apr 2007.
- 991 [11] T. M. Atanackovic and B. Stankovic. Generalized wave equation in nonlocal elasticity. *Acta*
992 *Mechanica*, 208(1-2):1–10, nov 2008.
- 993 [12] Teodor M. Atanacković, S. Pilipović, B. Stanković, and D. Zorica. *Fractional Calculus with*
994 *Applications in Mechanics: Wave Propagation, Impact and Variational Principles*. ISTE
995 Ltd., 2014.
- 996 [13] G.A. Ateshian and J.A. Weiss. Anisotropic hydraulic permeability under finite deformation.
997 *J. Biomech. Engng.*, 132:111004–1–111004–7, 2010.
- 998 [14] N. Bellomo and L. Preziosi. Modelling and mathematical problems related to tumor evolution
999 and its interaction with the immune system. *Mathematical and Computer Modelling*, 32(3-
1000 4):413–452, aug 2000.
- 1001 [15] L.S. Bennethum, M.A. Murad, and J.H. Cushman. Macroscale thermodynamics and the
1002 chemical potential for swelling porous media. *Transport in Porous Media*, 39(2):187–225,
1003 2000.
- 1004 [16] Haim Brezis. *Functional Analysis, Sobolev Spaces and Partial Differential Equations*. Springer
1005 New York, 2010.
- 1006 [17] Michael M. Bronstein, Joan Bruna, Yann LeCun, Arthur Szlam, and Pierre Vandergheynst.
1007 Geometric deep learning: Going beyond euclidean data. *IEEE Signal Processing Magazine*,
1008 34(4):18–42, jul 2017.
- 1009 [18] Alfonso Bueno-Orovio, David Kay, Vicente Grau, Blanca Rodriguez, and Kevin Burrage.
1010 Fractional diffusion models of cardiac electrical propagation: role of structural heterogeneity
1011 in dispersion of repolarization. *Journal of The Royal Society Interface*, 11(97):20140352, aug
1012 2014.
- 1013 [19] H. Byrne and L. Preziosi. Modelling solid tumour growth using the theory of mixtures.
1014 *Mathematical Medicine and Biology*, 20(4):341–366, dec 2003.

- 1015 [20] H.M. Byrne and M.A. Chaplain. Growth of nonnecrotic tumors in the presence and absence
1016 of inhibitors. *Mathematical biosciences*, 130:151–181, December 1995.
- 1017 [21] Silvia Capuani, Marco Palombo, Andrea Gabrielli, Augusto Orlandi, Bruno Maraviglia, and
1018 Francesco S. Pastore. Spatio-temporal anomalous diffusion imaging: results in controlled
1019 phantoms and in excised human meningiomas. *Magnetic Resonance Imaging*, 31(3):359–365,
1020 apr 2013.
- 1021 [22] A. Carpinteri, P. Cornetti, and A. Saporà. A fractional calculus approach to nonlocal elas-
1022 ticity. *The European Physical Journal Special Topics*, 193(1):193–204, mar 2011.
- 1023 [23] J.J. Casciari, S.V. Sotirchos, and R.M. Sutherland. Mathematical modelling of microenviron-
1024 ment and growth in EMT6/ro multicellular tumour spheroids. *Cell Proliferation*, 25(1):1–22,
1025 jan 1992.
- 1026 [24] Joseph J. Casciari, Stratis V. Sotirchos, and Robert M. Sutherland. Variations in tumor
1027 cell growth rates and metabolism with oxygen concentration, glucose concentration, and
1028 extracellular pH. *Journal of Cellular Physiology*, 151(2):386–394, may 1992.
- 1029 [25] M.A.J. Chaplain, L. Graziano, and L. Preziosi. Mathematical modelling of the loss of tissue
1030 compression responsiveness and its role in solid tumour development. *Mathematical Medicine
1031 and Biology: A Journal of the IMA*, 23(3):197–229, sep 2006.
- 1032 [26] A.S. Chaves. A fractional diffusion equation to describe lévy flights. *Physics Letters A*,
1033 239(1-2):13–16, feb 1998.
- 1034 [27] V. Ciancio, M. Dolfin, M. Francaviglia, and S. Preston. Uniform materials and the multi-
1035 plicative decomposition of the deformation gradient in finite elasto-plasticity. *J. Non-Equilib.
1036 Thermodyn.*, 33(3):199–234, 2008.
- 1037 [28] P. Ciarletta, M. Destrade, and A. L. Gower. On residual stresses and homeostasis: an elastic
1038 theory of functional adaptation in living matter. *Scientific Reports*, 6(1), apr 2016.
- 1039 [29] D Cioranescu. *An introduction to homogenization*. Oxford University Press, 1999.
- 1040 [30] S. Cleja-Tigoiu and G. A. Maugin. Eshelby’s stress tensors in finite elastoplasticity. *Acta
1041 Mechanica*, 139(1-4):231–249, mar 2000.
- 1042 [31] Helena L.E. Coker, Matthew R. Cheetham, Daniel R. Kattnig, Yong J. Wang, Sergi Garcia-
1043 Manyes, and Mark I. Wallace. Controlling anomalous diffusion in lipid membranes. *Biophys-
1044 ical Journal*, 116(6):1085–1094, mar 2019.
- 1045 [32] S. C. Cowin and G. A. Holzapfel. On the modeling of growth and adaptation. In Holzapfel G.
1046 A. and Odgen R. W., editors, *Mechanics of Biological Tissue*, pages 29–46. Springer-Verlag,
1047 2006.
- 1048 [33] E. Crevacore, S. Di Stefano, and A. Grillo. Coupling among deformation, fluid flow, struc-
1049 tural reorganisation and fibre reorientation in fibre-reinforced, transversely isotropic biological
1050 tissues. *International Journal of Nonlinear Mechanics*, In press, 2018.

- 1051 [34] Y. Danyuo, C. J. Ani, A. A. Salifu, J. D. Obayemi, S. Dozie-Nwachukwu, V. O. Obanawu,
1052 U. M. Akpan, O. S. Odusanya, M. Abade-Abugre, F. McBagonluri, and W. O. Soboyejo.
1053 Anomalous release kinetics of prodigiosin from poly-n-isopropyl-acrylamid based hydrogels
1054 for the treatment of triple negative breast cancer. *Scientific Reports*, 9(1), mar 2019.
- 1055 [35] D. del Castillo-Negrete. Fractional diffusion models of nonlocal transport. *Physics of Plasmas*,
1056 13(8):082308, aug 2006.
- 1057 [36] Zhi-Qiang Deng, Vijay P. Singh, and Lars Bengtsson. Numerical solution of fractional
1058 advection-dispersion equation. *Journal of Hydraulic Engineering*, 130(5):422–431, may 2004.
- 1059 [37] Mario Di Paola and Massimiliano Zingales. Long-range cohesive interactions of non-local
1060 continuum faced by fractional calculus. *International Journal of Solids and Structures*,
1061 45(21):5642–5659, oct 2008.
- 1062 [38] Mario Di Paola and Massimiliano Zingales. Fractional differential calculus for 3d mechanically
1063 based non-local elasticity. *International Journal for Multiscale Computational Engineering*,
1064 9(5):579–597, 2011.
- 1065 [39] A. DiCarlo and S. Quiligotti. Growth and balance. *Mechanics Research Communications*,
1066 29(6):449–456, nov 2002.
- 1067 [40] Nader Engheta. Fractional curl operator in electromagnetics. *Microwave and Optical Tech-*
1068 *nology Letters*, 17(2):86–91, feb 1998.
- 1069 [41] M. Epstein. Self-driven continuous dislocations and growth. In Maugin G.A. Steinmann P.,
1070 editor, *Mechanics of Material Forces. Advances in Mechanics and Mathematics*, volume 11,
1071 pages 129–139. Springer, Boston, MA, 2005.
- 1072 [42] M. Epstein and G.A. Maugin. Thermomechanics of volumetric growth in uniform bodies.
1073 *International Journal of Plasticity*, 16(7-8):951–978, jun 2000.
- 1074 [43] A. Cemal Eringen. Linear theory of nonlocal elasticity and dispersion of plane waves. *Inter-*
1075 *national Journal of Engineering Science*, 10(5):425–435, may 1972.
- 1076 [44] Gissell Estrada-Rodriguez, Heiko Gimperlein, Kevin J. Painter, and Jakub Stoczek. Space-
1077 time fractional diffusion in cell movement models with delay. *Mathematical Models and*
1078 *Methods in Applied Sciences*, 29(01):65–88, jan 2019.
- 1079 [45] N. Filipovitch, K. M. Hill, A. Longjas, and V. R. Voller. Infiltration experiments demon-
1080 strate an explicit connection between heterogeneity and anomalous diffusion behavior. *Water*
1081 *Resources Research*, 52(7):5167–5178, jul 2016.
- 1082 [46] G. Forgacs, R.A. Foty, Y. Shafrir, and M.S. Steinberg. Viscoelastic properties of living
1083 embryonic tissues: a quantitative study. *Biophysical Journal*, 74:2227–2234, 1998.
- 1084 [47] P. Fuschi, A. A. Pisano, and D. De Domenico. Plane stress problems in nonlocal elasticity:
1085 finite element solutions with a strain-difference-based formulation. *Journal of Mathematical*
1086 *Analysis and Applications*, 431(2):714–736, nov 2015.

- 1087 [48] Naama Gal and Daphne Weihs. Experimental evidence of strong anomalous diffusion in living
1088 cells. *Physical Review E*, 81(2), feb 2010.
- 1089 [49] Heiko Gimperlein and Jakub Stoczek. Space–time adaptive finite elements for nonlocal
1090 parabolic variational inequalities. *Computer Methods in Applied Mechanics and Engineering*,
1091 352:137–171, aug 2019.
- 1092 [50] C. Giverso and L. Preziosi. Modelling the compression and reorganization of cell aggregates.
1093 *Mathematical Medicine and Biology*, 29:181–204, 2012.
- 1094 [51] C. Giverso, M. Scianna, and A. Grillo. Growing avascular tumours as elasto-plastic bodies
1095 by the theory of evolving natural configurations. *Mech. Res. Commun.*, 68:31–39, 2015.
- 1096 [52] A. Goriely. *The Mathematics and Mechanics of Biological Growth*. Springer New York, 2016.
- 1097 [53] A. Grillo, M. Carfagna, and S. Federico. Non-Darcian flow in fibre-reinforced biological
1098 tissues. *Meccanica*, 52:3299–3320, 2017.
- 1099 [54] A. Grillo, S. Federico, and G. Wittum. Growth, mass transfer, and remodeling in fiber-
1100 reinforced, multi-constituent materials. *Int. J. Nonlinear Mech.*, 47:388–401, 2012.
- 1101 [55] A. Grillo, R. Prohl, and G. Wittum. A poroplastic model of structural reorganisation in
1102 porous media of biomechanical interest. *Continuum Mech. Therm.*, 28:579–601, 2016.
- 1103 [56] Alfio Grillo, Salvatore Di Stefano, Ariel Ramírez-Torres, and Michele Loverre. A study of
1104 growth and remodeling in isotropic tissues, based on the anand-aslan-chester theory of strain-
1105 gradient plasticity. *GAMM-Mitteilungen*, 42(4), may 2019.
- 1106 [57] Morton E. Gurtin. On the plasticity of single crystals: free energy, microforces, plastic-strain
1107 gradients. *Journal of the Mechanics and Physics of Solids*, 48(5):989–1036, may 2000.
- 1108 [58] Klaus Hackl and Franz Dieter Fischer. On the relation between the principle of maximum
1109 dissipation and inelastic evolution given by dissipation potentials. *Proceedings of the Royal
1110 Society A: Mathematical, Physical and Engineering Sciences*, 464(2089):117–132, oct 2007.
- 1111 [59] Kotaybah Hashlamoun, Ziad Abusara, Ariel Ramírez-Torres, Alfio Grillo, Walter Herzog,
1112 and Salvatore Federico. Fluorescence recovery after photobleaching: direct measurement of
1113 diffusion anisotropy. *Biomechanics and Modeling in Mechanobiology*, jun 2020.
- 1114 [60] S.M. Hassanizadeh. Derivation of basic equations of mass transp. porous med., part 2. gen-
1115 eralized darcy’s and fick’s laws. *Adv. Water Resour.*, 9:207–222, 1986.
- 1116 [61] Gabriel Helmlinger, Paolo A. Netti, Hera C. Lichtenbeld, Robert J. Melder, and Rakesh K.
1117 Jain. Solid stress inhibits the growth of multicellular tumor spheroids. *Nature Biotechnology*,
1118 15(8):778–783, aug 1997.
- 1119 [62] M.H. Holmes and V.C. Mow. The nonlinear characteristics of soft gels and hydrated connec-
1120 tive tissues in ultrafiltration. *Journal of biomechanics*, 23:1145–1156, 1990.

- 1121 [63] Quanzhong Huang, Guanhua Huang, and Hongbin Zhan. A finite element solution for the
1122 fractional advection-dispersion equation. *Advances in Water Resources*, 31(12):1578–1589,
1123 dec 2008.
- 1124 [64] J. D. Humphrey. Towards a theory of vascular growth and remodeling. In Holzapfel G.A.
1125 and Ogden R.W., editors, *Mechanics of Biological Tissue*, pages 3–15. Springer-Verlag, 2006.
- 1126 [65] Ruben Interian, Reinaldo Rodríguez-Ramos, Fernando Valdés-Ravelo, Ariel Ramírez-Torres,
1127 Celso Ribeiro, and Aura Conci. Tumor growth modelling by cellular automata. *Mathematics
1128 and Mechanics of Complex Systems*, 5(3-4):239–259, oct 2017.
- 1129 [66] R.K. Jain, J.D. Martin, and T. Stylianopoulos. The role of mechanical forces in tumor growth
1130 and therapy. *Annual Review of Biomedical Engineering*, 16:321–346, 2014.
- 1131 [67] Chongming Jiang, Chunyan Cui, Li Li, and Yuanzhi Shao. The anomalous diffusion of a
1132 tumor invading with different surrounding tissues. *PLoS ONE*, 9(10):e109784, oct 2014.
- 1133 [68] Ansgar Jüngel and Ines Viktoria Stelzer. Entropy structure of a cross-diffusion tumor-growth
1134 model. *Mathematical Models and Methods in Applied Sciences*, 22(07):1250009, may 2012.
- 1135 [69] M A Konerding, E Fait, and A Gaumann. 3d microvascular architecture of pre-cancerous
1136 lesions and invasive carcinomas of the colon. *British Journal of Cancer*, 84(10):1354–1362,
1137 2001.
- 1138 [70] R. Krishna and J.A. Wesselingh. The maxwell-stefan approach to mass transfer. *Chemical
1139 Engineering Science*, 52(6):861–911, mar 1996.
- 1140 [71] E. Kröner. Elasticity theory of materials with long range cohesive forces. *International
1141 Journal of Solids and Structures*, 3(5):731–742, sep 1967.
- 1142 [72] Ellen Kuhl. Growing matter: A review of growth in living systems. *J. Mech. Behav. Biomed.
1143 Mater.*, 29:529–543, jan 2014.
- 1144 [73] M. Köpf, C. Corinth, O. Haferkamp, and T.F. Nonnenmacher. Anomalous diffusion of water
1145 in biological tissues. *Biophysical Journal*, 70(6):2950–2958, jun 1996.
- 1146 [74] Daniel J. Lacks. Tortuosity and anomalous diffusion in the neuromuscular junction. *Physical
1147 Review E*, 77(4), apr 2008.
- 1148 [75] E. K. Lenzi, H. V. Ribeiro, A. A. Tateishi, R. S. Zola, and L. R. Evangelista. Anomalous
1149 diffusion and transport in heterogeneous systems separated by a membrane. *Proceedings of
1150 the Royal Society A: Mathematical, Physical and Engineering Sciences*, 472(2195):20160502,
1151 nov 2016.
- 1152 [76] V.E. Lynch, B.A. Carreras, D. del Castillo-Negrete, K.M. Ferreira-Mejias, and H.R. Hicks.
1153 Numerical methods for the solution of partial differential equations of fractional order. *Journal
1154 of Computational Physics*, 192(2):406–421, dec 2003.
- 1155 [77] P. Macklin, Vittorio Cristini, and John Lowengrub. Biological background. In *Multiscale
1156 Modeling of Cancer*, pages 8–23. Cambridge University Press, 2010.

- 1157 [78] Paul Macklin, Steven McDougall, Alexander R. A. Anderson, Mark A. J. Chaplain, Vittorio
1158 Cristini, and John Lowengrub. Multiscale modelling and nonlinear simulation of vascular
1159 tumour growth. *Journal of Mathematical Biology*, 58(4-5):765–798, sep 2009.
- 1160 [79] J.E. Marsden and T.J.R. Hughes. *Mathematical Foundations of Elasticity*. Dover Publica-
1161 tions, Inc., Mineola, New York, 1983.
- 1162 [80] P. Mascheroni, M. Carfagna, A. Grillo, D.P. Boso, and B.A. Schrefler. An avascular tumor
1163 growth model based on porous media mechanics and evolving natural states. *Mathematics
1164 and Mechanics of Solids*, 23(4):686–712, jun 2018.
- 1165 [81] P. Mascheroni, C. Stigliano, M. Carfagna, D.P. Boso, L. Preziosi, P. Decuzzi, and B.A.
1166 Schrefler. Predicting the growth of glioblastoma multiforme spheroids using a multiphase
1167 porous media model. *Biomech. Model. Mechanobiol.*, 15(5):1215–1228, jan 2016.
- 1168 [82] Mark M. Meerschaert, Jeff Mortensen, and Stephen W. Wheatcraft. Fractional vector calculus
1169 for fractional advection–dispersion. *Physica A: Statistical Mechanics and its Applications*,
1170 367:181–190, jul 2006.
- 1171 [83] Mark M. Meerschaert and Charles Tadjeran. Finite difference approximations for two-sided
1172 space-fractional partial differential equations. *Applied Numerical Mathematics*, 56(1):80–90,
1173 jan 2006.
- 1174 [84] Ralf Metzler and Joseph Klafter. The random walk’s guide to anomalous diffusion: a frac-
1175 tional dynamics approach. *Physics Reports*, 339(1):1–77, dec 2000.
- 1176 [85] M.V. Mićunović. *Thermomechanics of Viscoplasticity*. Springer New York, 2009.
- 1177 [86] Shlomo P. Neuman and Daniel M. Tartakovsky. Perspective on theories of non-fickian trans-
1178 port in heterogeneous media. *Advances in Water Resources*, 32(5):670–680, may 2009.
- 1179 [87] K. Nishimoto. *Fractional Calculus: Integrations and Differentiations of Arbitrary Order*.
1180 University of New Haven Press, 1989.
- 1181 [88] Keith B. Oldham and Jerome Spanier. *The Fractional Calculus. Theory and Applications of
1182 Differentiation and Integration to Arbitrary Order*. Elsevier Science, 1974.
- 1183 [89] P. Paradisi, R. Cesari, F. Mainardi, A. Maurizi, and F. Tampieri. A generalized fick’s law to
1184 describe non-local transport effects. *Physics and Chemistry of the Earth, Part B: Hydrology,
1185 Oceans and Atmosphere*, 26(4):275–279, jan 2001.
- 1186 [90] R. Penta and D. Ambrosi. The role of the microvascular tortuosity in tumor transport
1187 phenomena. *Journal of Theoretical Biology*, 364:80–97, jan 2015.
- 1188 [91] Raimondo Penta, Laura Miller, Alfio Grillo, Ariel Ramírez-Torres, Pietro Mascheroni, and
1189 Reinaldo Rodríguez-Ramos. Porosity and diffusion in biological tissues. recent advances and
1190 further perspectives. In *Constitutive Modelling of Solid Continua*, pages 311–356. Springer
1191 International Publishing, nov 2020.

- 1192 [92] Igor Podlubny. *Fractional Differential Equations: An Introduction to Fractional Derivatives,*
1193 *Fractional Differential Equations, to Methods of Their Solution and Some of Their Applica-*
1194 *tions (ISSN Book 198).* Academic Press, 1998.
- 1195 [93] Adrien Poulenard and Maks Ovsjanikov. Multi-directional geodesic neural networks via equiv-
1196 ariant convolution. *ACM Transactions on Graphics*, 37(6):1–14, dec 2018.
- 1197 [94] S. Preston and M. Elzanowski. Material uniformity and the concept of the stress space. In
1198 Bettina Albers, editor, *Continuous Media with Microstructure*, pages 91–101. Springer-Verlag
1199 Berlin Heidelberg, 1 edition, 2010.
- 1200 [95] L. Preziosi and G. Vitale. A multiphase model of tumor and tissue growth including cell
1201 adhesion and plastic reorganization. *Math. Models Methods Appl. Sci.*, 21(09):1901–1932,
1202 sep 2011.
- 1203 [96] Ariel Ramírez-Torres, Salvatore Di Stefano, Alfio Grillo, Reinaldo Rodríguez-Ramos, José
1204 Merodio, and Raimondo Penta. An asymptotic homogenization approach to the microstruc-
1205 tural evolution of heterogeneous media. *International Journal of Non-Linear Mechanics*,
1206 106:245–257, nov 2018.
- 1207 [97] Ariel Ramírez-Torres, Reinaldo Rodríguez-Ramos, Rainer Glüge, Julián Bravo-Castillero,
1208 Raúl Guinovart-Díaz, and Rocío Rodríguez-Sanchez. Biomechanic approach of a growing
1209 tumor. *Mechanics Research Communications*, 51:32–38, jul 2013.
- 1210 [98] E.K. Rodriguez, A. Hoger, and A.D. McCulloch. Stress-dependent finite growth in soft elastic
1211 tissues. *J. Biomech.*, 27:455–467, 1994.
- 1212 [99] John Paul Roop. Computational aspects of FEM approximation of fractional advection
1213 dispersion equations on bounded domains in \mathbb{R}^2 . *Journal of Computational and Applied*
1214 *Mathematics*, 193(1):243–268, aug 2006.
- 1215 [100] Tiina Roose, S. Jonathan Chapman, and Philip K. Maini. Mathematical models of avascular
1216 tumor growth. *SIAM Review*, 49(2):179–208, jan 2007.
- 1217 [101] S. Di Stefano, A. Ramírez-Torres, R. Penta, and A. Grillo. Self-influenced growth through
1218 evolving material inhomogeneities. *International Journal of Non-Linear Mechanics*, 106:174–
1219 187, 2018.
- 1220 [102] S. Sadik and A. Yavari. On the origins of the idea of the multiplicative decomposition of the
1221 deformation gradient. *Mathematics and Mechanics of Solids*, 22(4):771–772, oct 2017.
- 1222 [103] Sandro Salsa, Federico M. G. Vegni, Anna Zaretti, and Paolo Zunino. Elementi di analisi
1223 funzionale. In *UNITEXT*, pages 259–324. Springer Milan, 2009.
- 1224 [104] S. G. Samko, A. A. Kilbas, and O. I. Marichev. *Fractional Integrals and Derivatives: Theory*
1225 *and Applications.* Gordon and Breach Science Publishers, 1993.
- 1226 [105] A. Sapora, P. Cornetti, B. Chiaia, E. K. Lenzi, and L. R. Evangelista. Nonlocal diffusion
1227 in porous media: A spatial fractional approach. *Journal of Engineering Mechanics*, 143(5),
1228 may 2017.

- 1229 [106] Stefan C. Schonsheck, Bin Dong, and Rongjie Lai. Parallel transport convolution: A new
1230 tool for convolutional neural networks on manifolds. *arXiv preprint*, 2018.
- 1231 [107] G Sciumè, S Shelton, W G Gray, C T Miller, F Hussain, M Ferrari, P Decuzzi, and B A Schre-
1232 fler. A multiphase model for three-dimensional tumor growth. *New J. Phys.*, 15(1):015005,
1233 jan 2013.
- 1234 [108] Mihir Sen and Eduardo Ramos. A spatially non-local model for flow in porous media. *Trans-
1235 port in Porous Media*, 92(1):29–39, oct 2011.
- 1236 [109] S.L. Sobolev. Nonlocal diffusion models: Application to rapid solidification of binary mix-
1237 tures. *International Journal of Heat and Mass Transfer*, 71:295–302, apr 2014.
- 1238 [110] T. Stylianopoulos, J.D. Martin, V.P. Chauhan, S.R. Jain, and et al. Causes, conse-
1239 quences, and remedies for growth-induced solid stress in murine and human tumors. *PNAS*,
1240 109(38):15101–15108, 2012.
- 1241 [111] T. Stylianopoulos, J.D. Martin, M. Snuderl, F. Mpekris, S.R. Jain, and R.K. Jain. Coevolu-
1242 tion of solid stress and interstitial fluid pressure in tumors during progression: Implications
1243 for vascular collapse. *Cancer Research*, 73(13):3833–3841, apr 2013.
- 1244 [112] V. E. Tarasov and G. M. Zaslavsky. Fractional dynamics of systems with long-range interac-
1245 tion. *Communications in Nonlinear Science and Numerical Simulation*, 11(8):885–898, dec
1246 2006.
- 1247 [113] Vasily E. Tarasov. Fractional vector calculus and fractional maxwell’s equations. *Annals of
1248 Physics*, 323(11):2756–2778, nov 2008.
- 1249 [114] A. Tomic, A. Grillo, and S. Federico. Poroelastic materials reinforced by statistically oriented
1250 fibres — numerical implementation and application to articular cartilage. *IMA J. Appl.
1251 Math.*, 79:1027–1059, 2014.
- 1252 [115] P. R. Wills, D. J. Scott, and D. J. Winzor. Thermodynamics and thermodynamic nonideality.
1253 In G. C. K. Roberts, editor, *Encyclopedia of Biophysics*, pages 2583–2589. Springer, Berlin
1254 Heidelberg, 2013.